Chapter 5
Classical Helium Heat Transfer

Normal helium (He I) is a simple liquid with state properties that can be described reasonably well by classical models of the type introduced in Chap. 3. However, the dynamics of heat and mass transfer are of particular interest to engineering applications. Heat transfer, which is the subject of the present chapter, is probably the most important single characteristic of cryogenic fluids. The subject has considerable physical basis, and the models used to describe the phenomena are a combination of fundamental physics and engineering correlations. Pool boiling heat transfer is an often studied engineering problem related to cryogenic fluids including liquid helium. Pool boiling is a common term used to describe an experimental configuration consisting of a heater, either a plate or wire, immersed in a large bath of the fluid. Normally, the bath has such an extent that it is possible to assume it to be infinite in size relative to the heater sample. This problem is a classic in heat transfer research; although more complex configurations are needed to model true engineering systems. Heat transfer to forced flow helium is also an important topic as it relates to the design of heat exchangers and superconducting magnets. The fluid dynamics of forced flow helium was covered extensively in Chap. 4. Here we concentrate on the processes of heat exchange. Of course, in the case of forced flow helium the fluid dynamics problem and the heat transfer problem are not completely separable.

There are a number of general characteristics of He I which are worth noting in the context of heat transfer. First of all, it has a rather small thermal conductivity and large specific heat, suggesting that conduction heat transport is of little significance to the overall heat transfer picture. Particularly in the steady state, the heat transport is dominated by convection mechanisms.

The traditional approach to the interpretation of heat transfer is best suited for engineering applications. The general philosophy is to assume that the heat transfer process is too complicated to understand from basic principles. A specific problem requires solution of a complex set of equations which are only treatable in the simplest geometries. Therefore, engineering problems are scaled on the basis of dimensionless variables, which are functions of the properties of the system. It is then possible to construct non-dimensional relationships which when fit to

S.W. Van Sciver, *Helium Cryogenics*, International Cryogenics Monograph Series,
DOI 10.1007/978-1-4419-9979-5_5,

experimental data can be applied universally to other systems. The strength of this approach is in its relative ease of application. These dimensionless relationships have been explored extensively and their forms are available in the literature [1, 2]. Furthermore, the computation of the parameters for a given set of conditions allows straightforward predictions for experimental data. When carried out correctly, the correspondence between experiment and correlations is quite satisfactory. The essential ingredient to this approach is sufficient quantity of experimental data, not only for the particular fluid in question but also for other fluids with widely varying properties. This need must be satisfied to instill reasonable confidence in the particular correlation at hand. Fortunately, for most liquids this kind of ground work has already been laid and the behavior of He I is in satisfactory agreement with the accepted correlations. The quality of the agreement is in part the subject of the present chapter.

For problems of heat transfer, the most important dimensionless quantity to consider is the Nusselt number, Nu. It represents a dimensionless heat transfer coefficient defined by the relationship

$$\mathrm{Nu} = \frac{hL}{k_f} \tag{5.1}$$

where $h = q/(T_s - T_b)$, the heat transfer coefficient of the surface, T_s and T_b are the local surface and bath temperatures, k_f is the thermal conductivity of the fluid, and L is the characteristic length scale in the problem. In pool boiling, L is the dimension of the heater, that is, its diameter or width. In forced flow the length scale is the diameter of the tube or cylinder. As we will see below, the Nusselt number appears in correlations used to describe both free convection and forced convection heat transfer.

In the case of free convection and pool boiling heat transfer the two relevant dimensionless numbers are the Grashof number (Gr) and Prandtl number (Pr). The Grashof number indicates the ratio of buoyancy forces relative to viscous forces; it is represented by the relationship

$$\mathrm{Gr} = \frac{g\beta(T_s - T_b)L^3}{v^2} \tag{5.2}$$

where g is the acceleration of gravity, β is the bulk expansivity, and v is the kinematic viscosity. The Prandtl number, discussed in Chap. 3, is the ratio of the mass to thermal diffusivities of the fluid

$$\mathrm{Pr} = \frac{v}{D_{th}} = \frac{\mu C_p}{k} \tag{5.3}$$

where $D_{th} = k/\rho C_p$. For systems that are dominated by natural convection mechanisms, that is, with negligible forced flow, the Nusselt number is a function of these two numbers,

$$\mathrm{Nu} = \phi(\mathrm{Gr})\ \psi(\mathrm{Pr}) \tag{5.4}$$

where ϕ and ψ are functions that can be determined by the empirical correlation of data.

Most empirical correlations for natural convection are given in terms of the Rayleigh number, which is simply the product of the Grashof and Prandtl numbers,

$$\mathrm{Ra} \equiv \mathrm{Gr}\ \mathrm{Pr} = \frac{g\beta(T_s - T_b)L^3}{D_{th}\nu} \tag{5.5}$$

Simplified correlations can then be written in the form

$$\mathrm{Nu} = C\ \mathrm{Ra}^n \tag{5.6}$$

where C is an empirically determined parameter. The coefficient n is dependent mostly on the geometrical and flow conditions. For a vertically oriented plate in an open bath, $n = \frac{1}{4}$ and $\mathrm{C} = 0.59$ when the flow is laminar while $n = \frac{1}{3}$ and $\mathrm{C} = 0.1$ in the turbulent regime [2]. The type of heat transfer condition that exists in a particular system can be described by the corresponding value of the Rayleigh number. The critical Rayleigh number Ra_c defines the transition between these regimes. For flat plates, the transition between pure conduction and convection occurs for $\mathrm{Ra}_c \approx 10^3$, while the transition between laminar and turbulent convection heat transfer usually occurs for $\mathrm{Ra}_c \approx 10^9$. These concepts assume single-phase heat transfer and consequently are not applicable in heat transfer processes that involve change of phase.

5.1 Regimes of Heat Transfer

To obtain a better physical feeling for pool boiling heat transfer, it is helpful to consider a hypothetical experimental system. Such an experiment, shown in Fig. 5.1, consists of a flat heated plate with some arbitrary orientation exposed to an effectively infinite bath of liquid helium. The experiment consists of heating the plate from inside the insulated region and measuring the temperature difference between the bath and surface, ΔT_s, as it varies with heat flux q. There are a number of variables that affect the results in this experiment. Among these are bath temperature and pressure, surface orientation, physical characteristics of the heated surface including coatings, and frequency of heat flux. The general impact of these variables is described further below.

Given this experimental configuration, a measurement consists of determining a relationship between the heat flux q and ΔT_s. A typical example of such a relationship is shown in Fig. 5.2. There are principally three regimes of heat transfer as indicated in the figure: (1) natural convection, (2) nucleate boiling, and

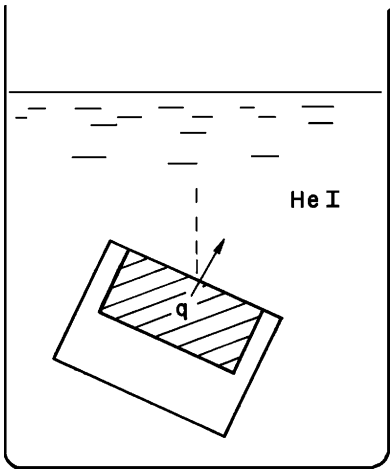

Fig. 5.1 Schematic of pool boiling heat transfer process from a planar surface of arbitrary orientation

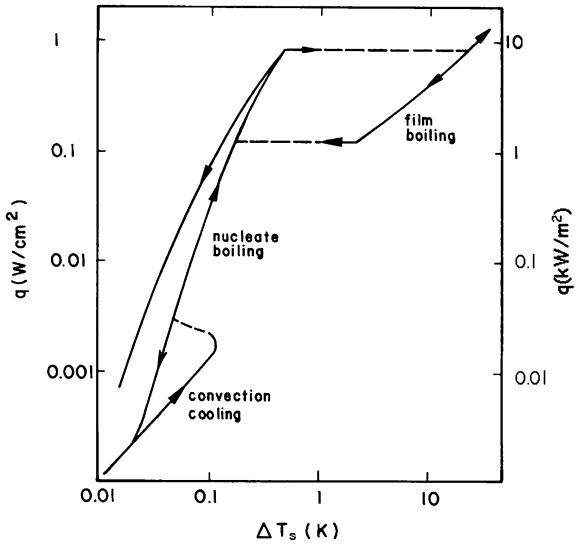

Fig. 5.2 Typical heat transfer relationship for pool boiling liquid

(3) film boiling. Each of these regimes has a characteristically different physical description, a schematic representation of which is shown in Fig. 5.3. At the lowest heat fluxes up to a few W/m^2, heat is transferred by natural convection; see Fig. 5.3a. No phase change is evident. This mechanism is characterized by density-driven convection currents near the heated surface. Surface temperature differences can be determined by the type of correlation given in (5.6). As the heat flux is increased, bubbles of helium vapor begin to form at preferred sites on the surface. These are typically surface imperfections. In the natural convection region, a certain amount of hysteresis in the heat transfer curve results from the activation and deactivation of these nucleation sites.

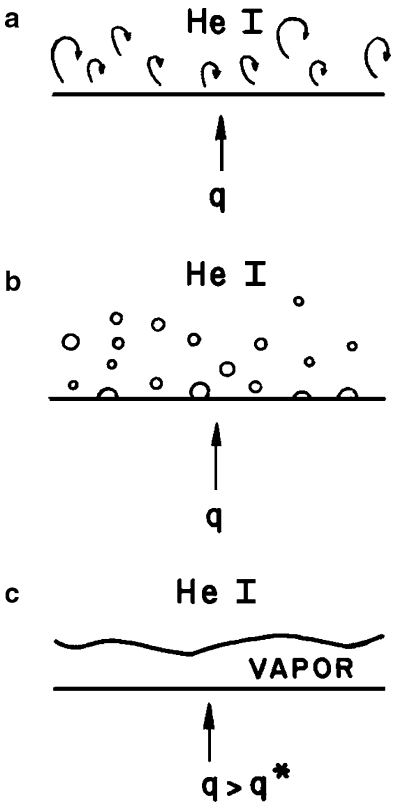

Fig. 5.3 Schematic representation of regimes of heat transfer: (**a**) natural convection, (**b**) nucleate boiling, and (**c**) film boiling

As the heat flux is increased further, the nucleation sites get fully activated, meaning that each site contains one bubble. At this point the surface is referred to as being "educated" since now increasing the heat flux only serves to accelerate the rate of bubble growth and detachment. In the nucleate boiling regime, Fig. 5.3b, there is a layer of superheated liquid adjacent to the heater surface. As a bubble detaches, cold liquid from above rushes down to cool the surface. This bubble growth and detachment causes macroscopic turbulence.

At still higher heat fluxes, the nucleate boiling bubbles get so large and are detaching at such a great rate that they become unstable and coalesce into a continuous vapor film; see Fig. 5.3c. The heat flux at which this occurs is referred to as the peak nucleate boiling heat flux q^*. This regime is called film boiling. The condition is unstable and causes hysteresis in the heat transfer curve, as shown by the upper region in Fig. 5.2. On decreasing the heat flux, it is necessary to go to a value lower than q^* for recovery to the nucleate boiling regime. This recovery value is referred to as the minimum film boiling heat flux q_{mfb} or recovery heat flux q_R. In the film boiling regime, the surface temperature difference is typically an order of magnitude higher than with nucleate boiling. The hysteresis in this regime of heat transfer is associated with the stability of a vapor film below a higher-density liquid.

Numerous factors affect these heat transfer characteristics. For example, the surface condition of the heat transfer sample can affect both the peak heat flux q^* and ΔT_s, in the nucleate boiling regime. It is possible to obtain variations in these quantities by as much as a factor of 2–3 between samples. The mechanism by which surface preparation affects the heat transfer characteristics is believed to be associated with the number of available nucleation sites.

Surface orientation has a profound effect on the heat transfer behavior. Variation of the surface orientation with respect to the gravitational force can cause significant changes in the heat flux and minimum film boiling heat flux. The highest values for both these quantities occur with the surface facing upward, because the buoyancy force aids bubble detachment. This argument supports the observed result that q^* and q_{mfb} are minimum with the surface facing downward.

The thermodynamic state of the liquid helium bath is also an important parameter in the heat transfer process. The bath temperature has a significant effect on various heat transfer parameters, particularly the peak nucleate boiling heat flux q^*. Similarly, the bath pressure affects these values, particularly when considering the subcooled or supercritical state. These variables can be taken into account through the changes in the helium properties with temperature and pressure.

The frequency with which the heat transfer event occurs is also important for both the peak heat flux and temperature difference. At low frequencies up to perhaps 10 Hz, the behavior does not deviate significantly from that of the steady-state process. Heat transfer is controlled largely by convection mechanisms. However, at higher frequencies approaching the kilohertz range there is insufficient time for the bubble nucleation to occur. Consequently, the behavior becomes dominated by simple heat diffusion in the liquid adjacent to the solid. Then temperature differences are caused by two physical mechanisms – the thermal conductivity of the helium and interfacial conductance (Kapitza conductance).

Finally, variations in geometry can have a profound effect on the heat transfer. Many engineering systems consist of channels, tubes, or other complex geometries, which are vastly different from the open infinite bath configuration. Such factors can cause differences in the heat transfer at least in part caused by the limited coolant volume. Some of the physical phenomena that can occur include heat-induced natural circulation and vapor locking in narrow channels. In the following sections, these issues will be discussed in further detail.

5.2 Convective Heat Transfer

At very low heat fluxes in liquid helium, $q \approx 1$ W/m^2, heat is transferred by a combination of conduction and convection. It is described by a heat transfer coefficient $h = q/\Delta T_s$, where h is only weakly dependent on ΔT_s. This regime of heat transfer has only limited technological application in liquid helium because the heat fluxes are quite small. However, the problems of low heat flux heat transfer and of transitions between conduction and convection do have fundamental physical

significance. Certain special cases of heat transfer fall in the general area of exactly soluble classical physics problems.

A good example of such a special interest is the problem of convection onset in a layer of fluid that is heated from below. The main difference between this problem and similar ones concerning pool boiling heat transfer is that the fluid layer is to have a thickness dimension d that enters into the problem in one of the dimensionalized parameters. This problem is referred to as Bénard convection and the instability associated with the transition is called the Rayleigh-Bénard instability. The transition is between conductive heat transfer and steady convection. As the heat flux is increased, the condition where the fluid is at rest carrying heat by conduction is transformed to that where a polygonal convective cell structure occurs. This type of structure has been observed in visual experiments with room temperature fluids. These flows exhibit regularity and structure that have inspired considerable theoretical research into the dynamics of small perturbations in fluids heated from below. Theoretical modeling is achievable because the disturbances are assumed to be sufficiently small that their description, at most, adds linear terms to the fluid equations.

The theoretical description of Bénard convection begins with the continuity equation and the equations for conservation of momentum and energy. The growth or decay of perturbations in the velocity and temperature fields is governed by the following linearized equations [3]:

$$\nabla \cdot \mathbf{v} = 0 \tag{5.7a}$$

$$\frac{\partial \mathbf{v}}{\partial t} = -\frac{1}{\rho_0}\nabla p + v\nabla^2 \mathbf{v} - \mathbf{g}\beta T \tag{5.7b}$$

$$\frac{\partial T}{\partial t} = D\nabla^2 T - w\gamma \tag{5.7c}$$

Solutions to these equations establish the regions of convection growth or decay. The boundary between these regions is defined by a "critical" Rayleigh number which effectively is a nondimensional temperature difference. The most interesting of the three equations is (5.7c) which describes the effect of motion on the temperature gradient. Without the second term, $w\gamma$, the expression is simply the heat diffusion equation. The parameter γ is defined as the undisturbed temperature gradient due only to conduction ($\gamma = q/k$). The physical meaning of the term $w\gamma$ is that of the motion generator. Heat is swept upward while the cold fluid returns. Heat conduction is necessary to generate the initial temperature gradient, but since mass flow is involved, viscosity enters to resist the growth of the perturbation.

The problem of Bénard convection in He I has been studied by a number of workers. Experimental measurements normally consist of determining the variation of the Nusselt number with the normalized Rayleigh number ($\mathrm{Ra}/\mathrm{Ra}_c$). For any fluid, the Nusselt number represents the ratio of the effective thermal conductivity to the actual thermal conductivity obtained without convection. Plotted in Fig. 5.4 is

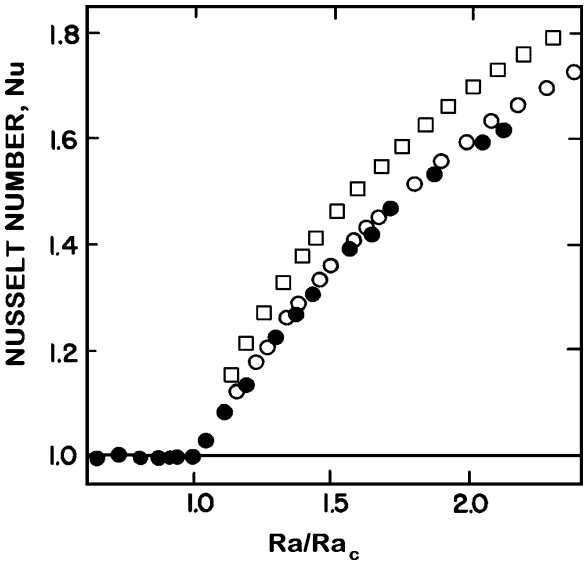

Fig. 5.4 Nusselt number as a function of Ra/Ra_c for Rayleigh-Bénard instability (From Behringer and Ahlers [4])

the normalized Nusselt number for one set of experiments on He I [4]. A number of interesting facts can be gleaned from these data. For example, above Ra_c the Nusselt number increases quite strongly with Ra. This is to be expected because the convection currents improve the heat transport. However, it is worth noting that the behavior of the Nu versus Ra/Ra_c plot appears to be somewhat universal in form. Slight differences in the data displayed in Fig. 5.4 are attributed to geometrical factors in the experiment.

The Rayleigh-Bénard instability is an interesting classical fluids problem. Its connection with helium heat transfer in practical configurations is limited, yet it does give fundamental insight into the fluid flow problem. As the heat flux is increased above about 0.1 W/m^2 bubbles begin to nucleate on the surface and simple convection is no longer the generally applicable solution. This problem is discussed in the next section.

Free convection heat transfer in cold helium gas is a more practically significant process because it can involve large heat fluxes. Helium near the critical point and in the supercritical regime has been studied fairly extensively [5–7]. Near the critical point, the heat transfer is seen to be enhanced considerably. For example, near 0.224 MPa, heat transfer coefficients as high as 100 kW/m^2 K have been observed. Such results correlate with the maxima in the thermodynamic properties near the critical point. Away from the critical point, the results are correlated best as a function of the Rayleigh number as (5.6). A reasonable fit to much of the helium data in this regime can be obtained from the expression [8],

$$Nu = 0.615\ Ra^{0.258} \tag{5.8}$$

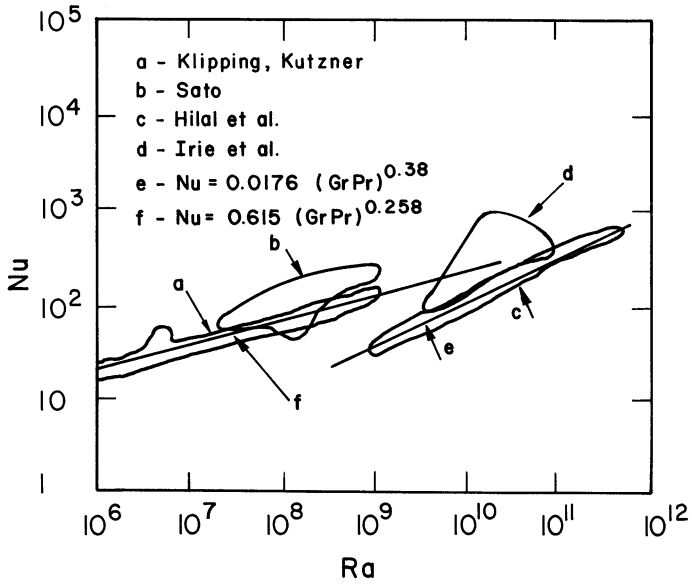

Fig. 5.5 Comparison of data and correlations on free convection heat transfer to supercritical helium (From Hilal [8])

which is close to the form expected for laminar free-convection heat transfer. A compilation of convective heat transfer results for supercritical helium is shown in Fig. 5.5 along with several correlations. There is a characteristic trend to the data; however, the agreement between various experiments is variable.

5.3 Nucleate Boiling Heat Transfer

Above a heat flux of a few W/m^2 in liquid helium the heat transfer surface begins to be covered with a large number of small vapor bubbles. This heat transfer process is quite different from that of natural convection because it is controlled mostly by the hydrodynamics of bubble growth and detachment rather than convection in the liquid.

Two conditions must exist at or near the heat transfer interface before there can be activation of bubble nucleation sites. First, there must be a boundary layer of liquid adjacent to the surface which is in the superheated condition. The thickness of this layer is determined by the thermal conductivity of the liquid, k, and the allowable superheat, $\Delta T_s = T_s - T_b$, where T_s is the maximum superheat temperature and T_b is the bath temperature. The thermal boundary layer thickness can therefore be written

$$\delta \approx \frac{k\ \Delta T_s}{q} \tag{5.9}$$

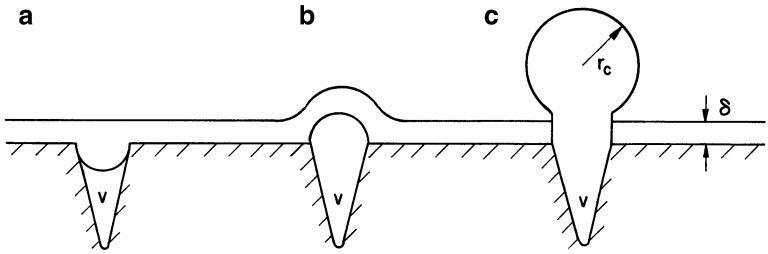

Fig. 5.6 Bubble nucleation on an imperfect surface: (**a**) negative radius of curvature, (**b**) positive radius of curvature, and (**c**) critical radius

Typically, δ is of the order of 1–10 μm for liquid helium near its normal boiling point.

Second, local surface imperfections must exist. These imperfections are necessary to provide preferential regions where bubbles can form. Shown schematically in Fig. 5.6, these imperfections usually are envisioned to be grooves or slots which allow a bubble to form with negative curvature, thus taking advantage of surface tension to stimulate the bubble nucleation. There are two principal reasons why the superheated boundary layer must form near the interface before substantial vapor nucleation can occur. First, the liquid near the interface is subcooled by the hydrostatic head ($\Delta p = \rho g h$) such that the local temperature must increase above ambient before the saturation condition can be attained. Second, and probably more important, in order to have vapor bubbles of positive radius of curvature, the surface tension of the liquid must be overcome.

5.3.1 Nucleation Theory

So far the discussion of nucleate boiling has been quite general and qualitative. However, it is worth considering two specific questions of quantitative nature. These concern the general vapor nucleation problem but are worked out as examples for the case of boiling liquid helium. The first question pertains to the growth of a vapor bubble on a nucleation site or actually anywhere in the bulk fluid. For a given amount of superheat, a bubble will be stable against the surface tension which is trying to collapse it. This problem involves consideration of the stability of a vapor bubble immersed in the bulk liquid – a case similar to that shown schematically in Fig. 5.6c.

The stability of a vapor bubble in the liquid can be evaluated in terms of the Clausius–Clapeyron equation. Considering the change of state between the liquid and vapor, thermodynamic stability requires that the vapor pressure derivative be given by

$$\left.\frac{dp}{dT}\right|_{sat} = \frac{\Delta s}{\Delta v} = \frac{h_{fg}}{T\ \Delta v} \tag{5.10}$$

where h_{fg} is the latent heat of the liquid and $\Delta v = v_g - v_l$ is the difference between the specific volumes of the vapor and liquid. For the interface of the bubble to be stable, it must have a pressure inside, p_v, which exceeds the local saturation pressure, p_s, by an amount related to the surface tension σ. For a spherical bubble, this requirement leads to the expression

$$p_v - p_s = \frac{2\sigma}{r} \tag{5.11}$$

where r is the local bubble radius. Obviously, the smaller the bubble the larger must be the pressure difference.

To get a feel for the order of magnitude of the quantities involved, assume that helium vapor obeys the ideal gas law and that the specific volume of the vapor is much greater than that of the liquid. These assumptions lead to the following approximation:

$$\Delta v \approx v_g \approx \frac{RT}{p} \tag{5.12}$$

Substituting (5.12) into (5.10) leads to a differential relationship

$$\frac{dp}{p} = \frac{h_{fg}}{R}\frac{dT}{T^2} \tag{5.13}$$

This expression must be integrated between saturation (T_s, p_s) and the condition inside the bubble (T_v, p_v) as determined by the stability relationship (5.11). Such a procedure yields a common relationship for the required vapor pressure within a bubble.

$$p_v = p_s e^{h_{fg}\Delta T_s/RT_s^2} \tag{5.14}$$

where a further approximation has been made that the temperature difference, $\Delta T_s = T_v - T_s$, is small compared to T_s.

The present discussion is aimed at determining the minimum radius of a stable vapor bubble in the bulk liquid. Substituting the expression for equilibrium of a vapor bubble (5.11) and allowing the radius to be undetermined, we obtain an expression for the critical radius,

$$r_c = \frac{2\sigma}{p_s}\left(e^{h_{fg}\Delta T_s/RT_s^2} - 1\right)^{-1} \tag{5.15}$$

which subsequently can be solved to determine the approximate value of r_c for any fluid.

Example 5.1

Calculate the critical radius for a vapor bubble in liquid helium at 4.2 K, 100 kPa. Assume that the vapor is superheated by 0.3 K. Estimate the number of helium molecules within the bubble.

Under the assumed conditions, $h_{fg} = 82$ J/mol and $\sigma = 0.15$ mJ/m^2 for a critical temperature difference assume $\Delta T \approx 0.3$ K. Inserting these numerical values into (5.15)

$$r_c = \frac{2\sigma}{p_s}\left(e^{h_{fg}\Delta T_s/RT_s^2} - 1\right)^{-1}$$

yields a critical radius $r_c \approx 16.4$ nm. The volume of the sphere is then,

$$V = \frac{4}{3}\pi r^3 = 1.8 \times 10^{-23}\text{m}^3$$

But the number density of helium molecules at 4.2 K is about 2.6×10^{27}/m^3 so the sphere contains approximately 10^4 atoms. It is reasonable to assume that the bubble containing this many molecules represents a thermodynamic system. Note that the above calculation is limited by the assumptions that $v_g \gg v_l$ and the ideal gas behavior for the vapor phase. These assumptions can lead to considerable inaccuracies in calculations of both the critical radii and the nucleation temperature.

The above calculation contains an assumed value for the superheat required to initiate the nucleation process, ΔT_s. Experimentally determined superheats actually vary by as much as half an order of magnitude. The highest values are obtained for the most ideal surfaces where nucleation is assumed to be homogeneous. These systems give nucleation superheats around 0.35 K at 4.2 K, 0.1 MPa. In fact, homogeneous nucleation superheat has been measured over the entire He I range and shown to agree with the empirical relationship [9]

$$\Delta T_s = 4.322\left(1 - \frac{T_b}{T_c}\right)^{1.534} \tag{5.16}$$

An expression can be derived for the homogeneous nucleation temperature based on a model suggested by Frenkel [10]. The analysis yields the rate of formation of bubbles having the critical radius r_c as defined by (5.11). As a function of the fluid properties, the rate is given by

$$R = n_l\left(\frac{\sigma}{m}\right)^{1/2}\exp\left(-\frac{4\pi}{3}\frac{\sigma\, r_c^2}{k_B T_s}\right) \tag{5.17}$$

where n_l is the number density in the liquid and m is the mass of a helium atom. The critical radius r_c is a function of the superheat ΔT_s, as well as other parameters such as absolute temperature T_s.

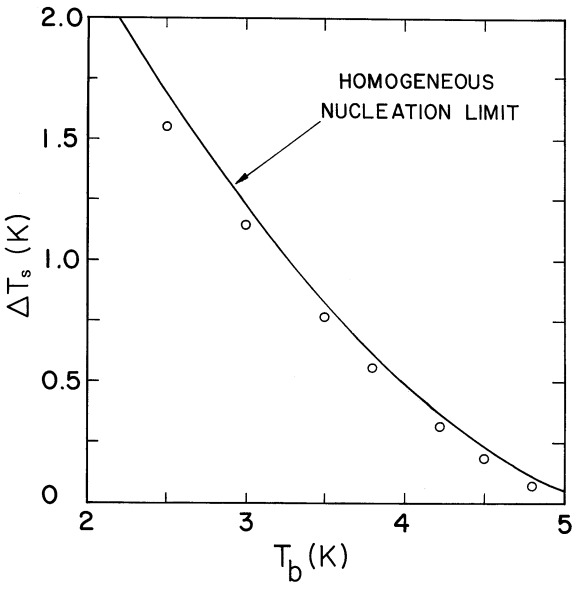

Fig. 5.7 Homogeneous nucleation limit for liquid helium heat transfer (From Flint and Van Cleve [11])

The expression given by (5.17) can be used to calculate the critical radius r_c or preferably the superheat ΔT_s. Such a calculation requires one arbitrary assumption: that of the reaction rate for the onset of nucleation. However, since the critical parameters enter into the exponential, the results are only weakly dependent on the choice of R. Typical values for this quantity are assumed to be 1 $cm^{-3} \cdot s^{-1}$. Furthermore, it is not possible to use the form developed above for the critical radius because the nonideality of the vapor phase plays an important role. Flint and Van Cleve [11] were able to obtain good agreement between experiment and theory if they used the actual behavior of the helium vapor pressure curve. The results of their calculation are shown in Fig. 5.7 along with experimental values for the nucleation superheat. These results were obtained on polished silicon chips oriented vertically in a bath of saturated liquid helium. The critical temperature differences are determined by noting the point where the hysteresis ended in a q versus ΔT curve; see Fig. 5.2. These data indicate a close correspondence between homogeneous nucleation theory and experiment. Typically, nucleation temperatures on real roughened surfaces are lower than those indicated in Fig. 5.7.

5.3.2 Heat Transfer Correlations

Once nucleation has occurred and the bubbles are large enough to be stable against collapse in the bulk fluid, the heat transfer becomes dependent on the hydrodynamics of bubble detachment and growth. To model the nucleate boiling heat transfer in this regime, it is necessary to know a number of quantities including

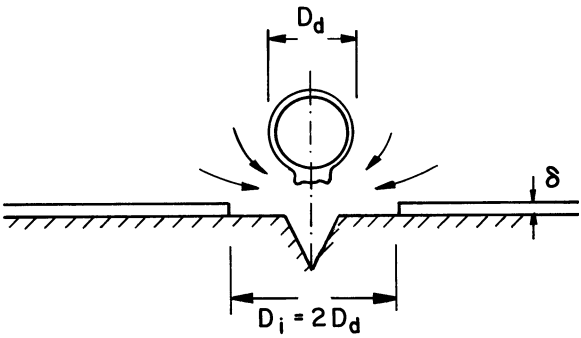

Fig. 5.8 Schematic of departing bubble and area of superheated liquid (From Bald [13])

the rate of bubble growth, frequency of detachment, and something of the hydrodynamics of the two-phase fluid consisting of the liquid in the vicinity of the bubble. A conceptual picture of the hydrodynamics of an individual bubble is beneficial in understanding the heat transfer mechanisms.

In the vicinity of the nucleation site, it was observed by Hsu and Graham [12] that a departing bubble took with it an area of superheated liquid equal to approximately twice the projected area of the bubble. Based on this hypothesis, shown schematically in Fig. 5.8, it is possible to account for the heat removed by one bubble as a sum of two quantities [13]

$$q_b = \frac{4\pi}{3} h_{fg} \rho v \int_A nfr_b^3 \, dA + 2\pi \Delta T_s C_l \rho_l \delta \int_A nfr_b^2 \, dA \tag{5.18}$$

where n is the number of nuclei per unit area of surface and the integrals are over the entire heat transfer surface area. The first quantity on the right-hand side is that due to the latent heat of the helium within the bubble, while the second is the heat required to superheat a new layer of liquid that replenishes the layer taken away with the departing bubble. The difficulties associated with applying (5.18) to real problems are multifold. First, the frequency of detachment f is involved with both terms in (5.18). The heat flux is proportional to f, which is largely an experimental quantity. The quantity is dependent on n, the number of nucleation sites per area, and r_c, the critical size of a departing bubble. The amount of superheat ΔT_s also enters (5.18) in the second term. In principle, this quantity can be determined from (5.17); however, for real surfaces it can vary considerably.

An additional complication enters when attempting to determine the total heat transferred in the nucleate boiling regime. In an actual process, there are two heat transfer terms: one due to bubble hydrodynamics, q_b, and one due to natural convection in the bulk fluid, q_{nc}:

$$q_{nb} = q_b + q_{nc} \tag{5.19}$$

There may be an additional contribution due to the interaction between natural convection and boiling, but it is unclear what form it would take. It is tempting to

neglect the natural convection term, assuming it is small; however, this is not always possible. Except in very special geometries, it is not possible to determine q_{nc} exactly. Therefore, engineering correlations are needed to describe the second term in (5.19). In general, the natural convection heat transfer can be written as a function of the dimensionless Rayleigh number as given by (5.6).

The above analysis has the potential of being able to describe the heat transfer in the nucleate boiling region. However, difficulty arises when determining the variables that enter (5.18) and (5.19). These variables mostly include the functional form of the natural convection, the amount of superheat ΔT_s, the bubble density n, and detachment frequency f. Since this analysis has limited practical usefulness, the preferred approach is to characterize the total heat transfer in terms of an engineering correlation.

The most popular and probably the best correlation used to describe the nucleate boiling regime is due to Kutateladze [14]. It is based on theory and experimental scaling of heat transfer to many different fluids:

$$\frac{h}{k_l}\left(\frac{\sigma}{g\rho_l}\right)^{1/2} = 3.25\times 10^{-4}\left[\frac{qC_{pl}\rho_l}{h_{fg}\rho_v k_l}\left(\frac{\sigma}{g\rho_l}\right)^{1/2}\right]^{0.6} \times\left[g\left(\frac{\rho_l}{\mu_l}\right)^2\left(\frac{\sigma}{g\rho_l}\right)^{3/2}\right]^{0.125}\left(\frac{p}{(\sigma g\rho_l)^{1/2}}\right)^{0.7} \tag{5.20}$$

where g is the acceleration of gravity and h_{fg} is the latent heat of vaporization. Although (5.20) is a complex expression, it does predict a reasonably correct functional dependence for the nucleate boiling heat transfer. Rearranging (5.20) into a more manageable form leads to the relationship

$$q = 1.90\times 10^{-9}\left[g\left(\frac{\rho_l}{\mu_l}\right)^2\chi^3\right]^{0.3125}\left(\frac{p\chi}{\sigma}\right)^{1.75}\left(\frac{\rho_l}{\rho_v}\right)^{1.5} \times\left(\frac{C_{pl}}{h_{fg}}\right)^{1.5}\left(\frac{k_l}{\chi}\right)(T_s - T_b)^{2.5} \tag{5.21a}$$

where

$$\chi = \left(\frac{\sigma}{g\rho_l}\right)^{1/2} \tag{5.21b}$$

and T_s and T_b are the surface and bath temperatures, respectively. The expression given by (5.21) is evaluated more easily. For the case of He I at 4.2 K, 0.1 MPa, the coefficient of proportionality can be calculated to equal 58 kW/m^{2}K^5.

The Kutateladze correlation is in reasonable accord with experimental measurements of heat transfer in He I. However, there is a wide variation in experimental

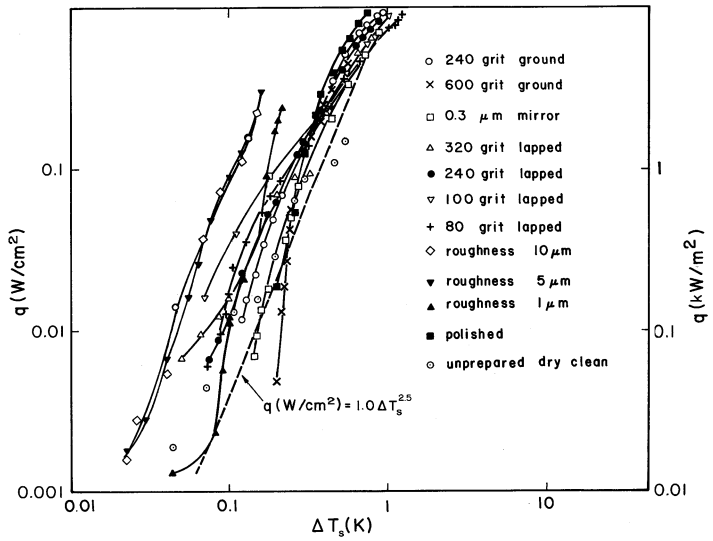

Fig. 5.9 Nucleate boiling heat transfer to He I (Compilation of data and suggested correlation from Schmidt [16])

data owing to the differences in sample preparation and surface material and orientation [15]. It is not too surprising, based on the hydrodynamic arguments above, that different surface preparations would yield much different results.

Figure 5.9 is a compilation of nucleate pool boiling data for flat copper surfaces facing upward and experiencing an increasing heat flux. The data vary over at least half an order of magnitude in ΔT with the smoothest surfaces apparently allowing a larger superheat. The larger superheat seen in smooth surfaces is consistent with the homogeneous nucleation arguments presented at the beginning of this section. Finally, note that an empirical fit used by Schmidt [16] to describe the data is also plotted in Fig. 5.9. This fit, which is quite close to the Kutateladze correlation with the exception of the coefficient of proportionality, is a conservative form useful for engineering applications.

5.3.3 *Maximum Nucleate Boiling Heat Flux*

The qualitative picture applied to the understanding of the maximum heat flux in pool boiling He I is as follows. Imagine a surface populated with a number of nucleation sites. At high heat fluxes, these sites are actively nucleating bubbles that grow to a stable size and detach at a frequency f controlled by buoyancy forces. With increasing heat flux, the number and size of these bubbles grow until a point is reached where they cover a sizable fraction of the heater surface. At this point, the individual bubbles are no longer the lowest-energy condition. They will prefer

to coalesce into a continuous vapor film which will blanket the entire heat transfer surface. This condition usually is referred to as the onset of film boiling. The difficulty is in being able to understand and predict the value of heat flux at which this event occurs, q^*.

To obtain some physical feeling for the occurrence of the maximum heat flux, consider an idealized surface facing upward as in Fig. 5.3b. The vapor bubbles are departing at velocity $\mathbf{v}_v$ while the replenishing liquid moves in the opposite direction at velocity $\mathbf{v}_l$. These velocities are not independent variables because the heat flow is determined by the rate of growth and departure of the vapor bubbles.

The hydrodynamics of this process is described by the Helmholtz instability [17], which pertains to the critical velocity of immiscible fluids moving relative to each other. Assume the liquid and vapor phases represent these two immiscible fluids. Then the boundary separating the two fluids would show an upward-moving vapor and downward-moving liquid. For these two fluids to pass each other undisturbed, the boundary that separates them must remain stable. The stability of this boundary is a function of a number of parameters including the relative velocities and densities of the two fluids. This is believed to be the condition that imposes the peak heat flux limit in classical liquids including He I.

Because of the relative motion of each fluid, there can be a surface wave set up at the interface. The velocity of this wave, c_s, is dependent on a number of factors including the surface tension and properties of the individual phases. The relationship for the surface wave velocity is

$$c_s^2 = \frac{\sigma m}{\rho_l + \rho_v} - \frac{\rho_l \rho_v}{(\rho_l + \rho_v)^2}(\mathbf{v}_v - \mathbf{v}_l)^2 \tag{5.22}$$

where $m = 2\pi/\lambda$ is the wave number of the surface wave. Since (5.22) consists of a difference between two positive quantities, it is possible for c_S^2 to have either a positive or negative value. For $c_S^2 > 0$ the surface wave can exist. If $c_S^2 > 0$ the surface wave velocity is imaginary, implying an instability in the interface. Therefore, the condition for maximum vapor velocity is obtained by equating c_S^2 to zero. Using conservation of mass flow, that is, $\rho_v \mathbf{v}_v + \rho_l \mathbf{v}_l = 0$, a simple expression is obtained:

$$\mathbf{v}_v^* = \left(\frac{\rho_l \sigma m}{\rho_v (\rho_l + \rho_v)} \right)^{1/2} \tag{5.23}$$

If the vapor velocity exceeds the value given by (5.23) there should be an unstable two-phase flow. The result is destruction of the interface between the two phases, which in turn leads to a condition where the vapor film blankets the heat transfer surface. This condition occurs at the maximum heat flux.

Zuber et al. [18] used the above reasoning to predict analytically the maximum heat flux q^*. Assuming that the heat is transported primarily by the vapor velocity and that the latent heat of the liquid that goes into the formation of the bubble is the

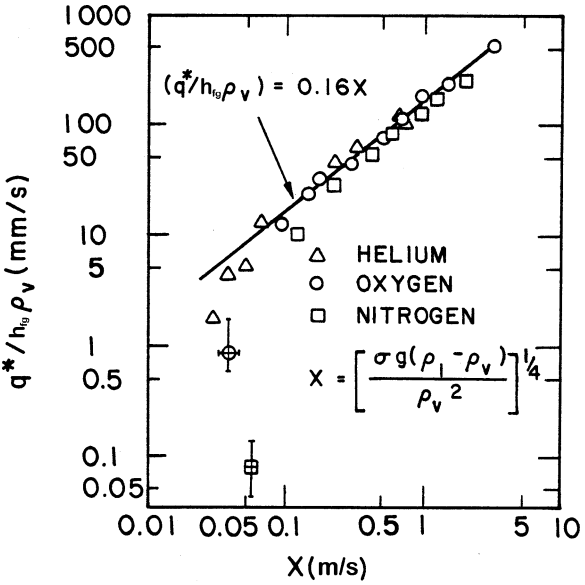

Fig. 5.10 Comparison of peak nucleate boiling heat fluxes with Kutateladze correlation (From Lyon [20])

dominant energy, Zuber and coworkers argued that the maximum heat flux can be written as a product of these quantities, that is,

$$q* = Kh_{fg}\rho_v\left(\frac{\sigma(\rho_l-\rho_v)g}{\rho_v^2}\right)^{1/4}\left(\frac{\rho_l}{\rho_l+\rho_v}\right)^{1/2} \tag{5.24}$$

where K is a numerical factor which in the case under consideration has a value of $\pi/24$. It is possible to derive a similar relationship for q^* from dimensionless group analysis. Based on experimental evidence, a similar relationship has developed acceptance [19, 20] that is,

$$q* = 0.16h_{fg}\rho_v^{1/2}[\sigma g(\rho_l-\rho_v)]^{1/4} \tag{5.25}$$

which is in close agreement with (5.24) with the exception of the last factor. The numerical factor in (5.25) is determined by correlation of numerous experimental results. For a numerical comparison, (5.25) predicts for liquid helium at 4.2 K, 0.1 MPa a value of $q^* = 8.5$ kW/m^2, which is in reasonable agreement with experimental results ranging from 5 kW/m^2 to around 15 kW/m^2. However, to test the relationship represented by (5.25) for a particular fluid, it is necessary to make measurements over a wide range of vapor densities or temperatures. Furthermore, to determine whether the correlation is universally acceptable, measurements of q^* for a variety of fluids are required. These experimental investigations determine the empirical constant of proportionality. Plotted in Fig. 5.10 are normalized measurements of $q^*/h_{fg}\rho_v$ versus the density function given in (5.25) [20]. Reasonable agreement with the correlation is seen for the three cryogenic fluids considered.

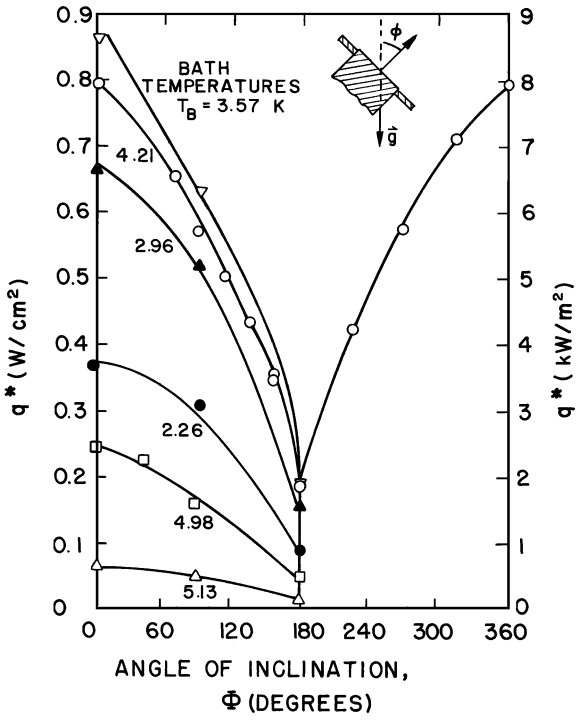

Fig. 5.11 Orientation dependence to the nucleate boiling heat flux (From Lyon [20])

It is worthwhile considering the temperature and orientation dependencies of q^* in comparison to (5.25). At high temperatures, q^* would be expected to decrease because as the critical point is approached there is no phase change associated with boiling and the latent heat vanishes. The theoretical expression indicates that the peak heat flux should go as the latent heat times the fourth root of the density difference. Both quantities vanish at the critical point. At low temperatures the latent heat approaches a constant and the temperature dependence is determined by the square root of the vapor density, which in turn decreases with temperature. Therefore, there should be a maximum in the peak heat flux. Analogous although somewhat less successful arguments can be used to describe the orientation dependence of q^*. Since the peak heat flux is proportional to the square root of the gravitational acceleration g, the buoyancy effects should decrease as the surface is turned from facing upward to facing downward. In fact, based on this simple argument, a surface facing downward should have $q^* = 0$. Experimentally, q^* obtains a minimum value a 180° orientation although its value is considerably greater than zero.

Measurements of the temperature and orientation dependence of q^* have been conducted most comprehensively by Lyon [20]. The orientation dependence of the maximum nucleate boiling heat flux is shown in Fig. 5.11. Note that for these experiments $q^* = 8$ kW/m^2 at 4.2 K which is quite close to the theoretical prediction. Furthermore, for each orientation there is a maximum value in the temperature dependence of q^*. Experimentally, this maximum occurs around 3.6 K. Finally, the

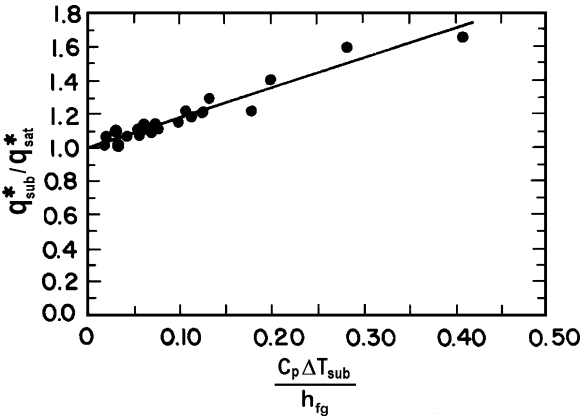

Fig. 5.12 Variation of the peak nucleate boiling heat flux with subcooling (From Ibrahim et al. [21])

orientation dependence is in qualitative agreement with theory. A minimum in q^* does occur at $\theta = 180°$, that is facing downward. However, the value of q^* at $\theta = 180°$ is still quite sizable, being about 25% of q^* for $\theta = 0°$.

The above correlations do not apply when the helium is subcooled to a state substantially off the saturated vapor pressure curve. In this case there can be no coexisting vapor. Some work [21–23] on the effect of subcooling on heat transfer has attempted to treat the peak heat flux correlation in terms of a subcooled temperature difference ΔT_{sub}. The subcooled temperature difference is defined as the difference between the bath temperature T_b and the temperature corresponding to saturation T_{sat}. As heat is applied from the heat transfer surface, the temperature rises. However, in subcooled He I a larger temperature difference is required than in saturated He I. This is due to the need to bring the local environment first to saturation followed by the amount of superheat needed to initiate nucleate boiling. Therefore, the absolute temperature needed to cause boiling at a given pressure should be independent of bath temperature. Such a hypothesis leads to a correlation for the enhancement of peak heat flux q^* with subcooling

$$\frac{q^*_{\text{sub}}}{q^*_{\text{sat}}} = 1 + \frac{aC_p \Delta T_{\text{sub}}}{h_{fg}} \tag{5.26}$$

where a is an empirical parameter found to be close to 1.75. Comparison of experimental results with the correlation given by (5.26) are shown in Fig. 5.12. Agreement is reasonable although the theory has received only limited application.

5.4 Film Boiling

Once the film boiling condition has been established, normally by exceeding q^* under steady-state conditions, a wholly different heat transfer process takes place. In the vicinity of the heat transfer interface the helium takes on a stable two-phase

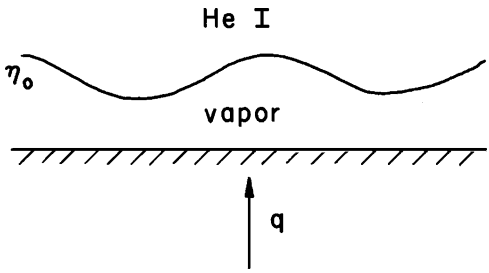

Fig. 5.13 Idealized film boiling heat transfer process

condition with a thin vapor layer blanketing the surface from the He I bath. For a surface facing upward, this condition is gravitationally unstable since the density of the liquid is considerably greater than that of the vapor. Experimentally, it is found that return to the nucleate boiling state requires a decrease in heat flux to q_R or q_{mfb}, which can be substantially less than q^* for most configurations. It follows that there are two principal issues that should be addressed when evaluating the film boiling state. First, given the conditions of film boiling, how is the recovery process explained? In particular, is it possible to predict q_R? This process has to do with the stability of the He I–vapor interface. The second question pertains to the need to correlate the heat transfer coefficient in the film boiling condition. This process normally relies on dimensionless group analysis developed for other liquids.

5.4.1 Minimum Film Boiling Heat Flux

The stability of the vapor film blanketing the heat transfer surface can be evaluated in terms of a hydrodynamic condition referred to as the Taylor instability [17]. This interpretation is a standard approach to treating the interface between two dissimilar fluids. Imagine the condition shown in Fig. 5.13 which is an idealized film boiling heat transfer process. The liquid helium is heavier than the vapor so it would prefer to rewet the surface; however, it is being maintained in the present condition by the high-temperature vapor film. The stability of the liquid-vapor interface is controlled by the behavior of surface wave oscillations. The wave can be assumed to have an amplitude η_0, and a wavelength λ. Surface waves must be damped for the interface to be stable, otherwise the amplitude would grow beyond the vapor film thickness and rewet the surface. It is therefore reasonable to construct a model based on the assumption that the stability of these waves controls the recovery process.

To be more quantitative about the above argument, assume that the stability of a surface wave is assured if the energy associated with surface tension exceeds the combination of the kinetic and potential energies in the wave. Both these terms are related to the amplitude of the surface oscillation η_0, as well as physical parameters

such as densities and surface tension. The kinetic and potential energies can be related as

$$\left.\frac{E}{\tilde{\lambda}}\right|_{KP} = \frac{g(\rho_l + \rho_v)\eta_0^2}{2} \tag{5.27}$$

where $\tilde{\lambda}$ is the wavelength of the surface oscillation and g is the gravitational acceleration. Similarly, the surface term can be written

$$\left.\frac{E}{\tilde{\lambda}}\right|_{\sigma} = \frac{1}{\tilde{\lambda}} \int_0^{\tilde{\lambda}} \Delta p \; \eta \; dx \tag{5.28}$$

where Δp is taken to be the pressure difference and η is a sinusoidal varying wave, that is $\eta = \eta_0 \sin 2\pi x/\tilde{\lambda}$. By integrating over the wavelength of the oscillation and using the approximation that the surface wave oscillation is small compared to $\tilde{\lambda}$, we can evaluate the integral (5.28):

$$\left.\frac{E}{\tilde{\lambda}}\right|_{\sigma} = \frac{4\pi\sigma\eta_0^2}{\tilde{\lambda}^2} \tag{5.29}$$

As already stated, the condition for stability demands that the surface energy exceed the dynamic energy. This leads to a condition on $\tilde{\lambda}$ by demanding that (5.29) not exceed (5.27), that is,

$$\tilde{\lambda} < 2\pi \left(\frac{2\sigma}{g(\rho_l - \rho_v)}\right)^{\frac{1}{2}} \tag{5.30}$$

For liquid helium near 4.2 K, (5.30) is obeyed for wavelengths less than about 2 mm, a dimension that must be comparable to a characteristic distance in the heat transfer problem, for example, the typical bubble dimension.

The minimum film boiling heat flux q_R can be understood by application of the Taylor instability theory to the film boiling heat transfer condition. Lienhard and Wong [24] and Zuber [18] used this analysis, identifying the breakdown of film boiling with the amplitude of the surface wave. The general relationship has one empirical constant and an explicit diameter dependence. For the special case of a flat plane, the correlation is simplified considerably:

$$q_R = 0.16 \; h_{\mathrm{fg}} \rho_v \left(\frac{g\sigma(\rho_l - \rho_v)}{(\rho_l + \rho_v)^2}\right)^{1/4} \tag{5.31}$$

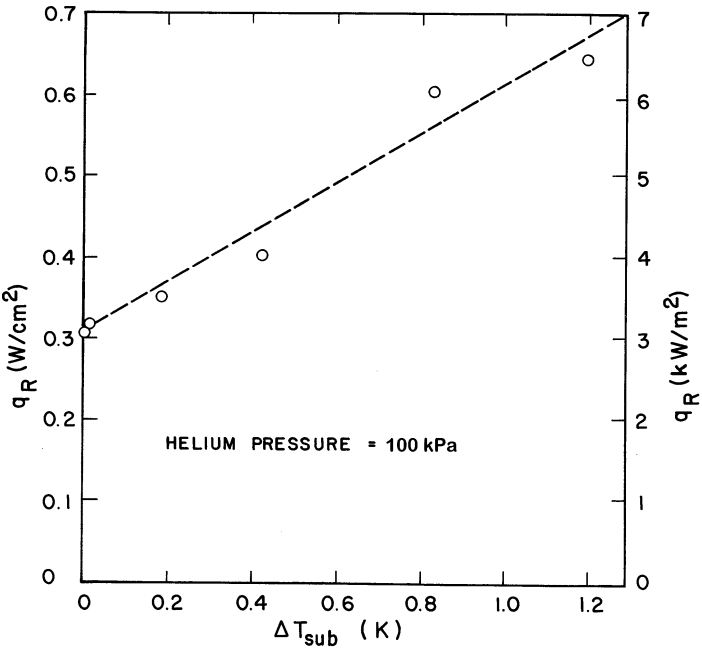

Fig. 5.14 Minimum film boiling heat flux for subcooled He I (from Ibrahim et al. [21])

It is interesting to compare (5.31) with (5.24), which predicts the peak heat flux q^*. Taking a ratio of these two expressions, the only important parameters turn out to be the relative densities of the liquid and vapor,

$$\frac{q_R}{q^*} = \left(\frac{\rho_v}{\rho_l + \rho_v}\right)^{1/2} \tag{5.32}$$

For example, considering liquid helium at 4.2 K, we find that the ratio described by (5.32) has a value of 0.35 at atmospheric pressure. Therefore, assuming $q^* = 8.5$ kW/m^2 as measured by Lyon [21] we find that (5.32) predicts a minimum film boiling heat flux of about 3 kW/m^2 in close agreement with experimental measurements.

The pressure dependence of the recovery heat flux is worth considering in light of the noted behavior of $q^*(p)$. As was observed in the previous section, subcooling increases q^* by about 50% per degree of ΔT_{sub} near atmospheric pressure. The subcooling effect on q_R is greater, as can be seen in Fig. 5.14. Note that q_R increases by about 90% per degree of ΔT_{sub} near atmospheric pressure [18]. The correlating relationships for the minimum film boiling heat flux predict this effect. Subcooling increases the ratio of the vapor to liquid density at saturation, which would result in an increase in q_R/q^*, as observed by experiment.

5.4.2 Heat Transfer Correlations

Once stable film boiling is established, it is of interest to be able to predict the magnitude of the film boiling heat transfer coefficient h_{fb} or the rate of heat flux q_{fb} for a given ΔT. Experimentally, h_{fb} has values that range over more than an order of magnitude between about 0.3 kW/m^2 K and nearly 10 kW/m^2 K, with the latter being achieved for fine wires with diameters of ~10 μm. The film boiling heat transfer also depends on fluid properties, being a function of the vapor and liquid densities, latent heat, and surface tension σ.

A number of semi-empirical correlations exist for prediction of heat transfer on the film boiling condition. The best known and perhaps most accepted of those is due to Breen and Westwater [25]. As in the case of the minimum film boiling heat flux q_R, these authors base their theory on the Taylor instability. They consider the wavelength condition given by (5.30) as the minimum required to release vapor bubbles into the bulk fluid from the boiling film. The correlation depends on the thermal properties of the fluid including specific heat and viscosity in addition to geometrical conditions such as the diameter of the heat transfer sample. The correlation relates the film boiling heat transfer coefficient to these quantities and a number of numerical constants:

$$h_{fb}\left(\frac{\sigma}{g(\rho_l-\rho_v)}\right)^{1/8}\left(\frac{\mu_v(T_s-T_b)}{k_v^3\rho_v(\rho_l-\rho_v)g\lambda'}\right)^{1/4} = 0.37+0.28\left(\frac{\sigma}{gD^2(\rho_l-\rho_v)}\right)^{1/2} \tag{5.33a}$$

where

$$\lambda' = \frac{\left[h_{fg}+0.34C_{p_v}(T_s-T_b)\right]^2}{h_{fg}} \tag{5.33b}$$

and represents an effective latent heat. T_s and T_b are the surface and bath temperatures, respectively. D is the diameter of the heater surface, which for film boiling has an effect on the heat transfer coefficient. For the special case where the heater diameter is greater than a few millimeters, the second term on the right-hand side is small and (5.33) may be approximated by the relationship

$$h_{fb} = 0.37\left(\frac{g(\rho_l-\rho_v)}{\sigma}\right)^{1/8}\left(\frac{k_v^3\rho_v(\rho_l-\rho_v)g\lambda'}{\mu_v(T_s-T_b)}\right)^{1/4} \tag{5.34}$$

Furthermore, in helium for moderate temperature differences, that is $\Delta T \gtrsim 5$ K, the second term in (5.33b) is dominant. Under these conditions, it can be shown easily that film boiling heat transfer $q \approx (T_s-T_b)^{3/4}$.

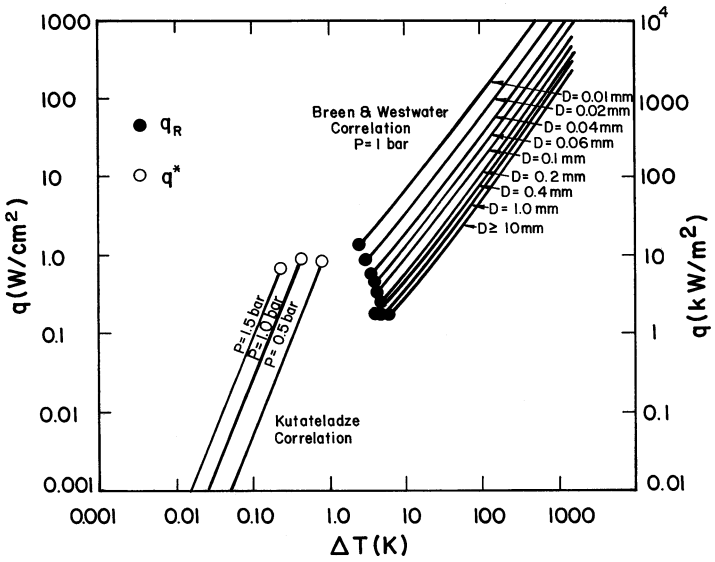

Fig. 5.15 A summary of pool boiling heat transfer correlations for He I

In summary, Fig. 5.15 is a plot of the various predictive relationships for nucleate and film boiling heat transfer [26]. A Comparison between data for nucleate boiling and minimum film boiling has been made already. For the case of film boiling heat transfer, the Breen–Westwater correlation is only moderately successful a predicting experimental data [19]. In general, film boiling heat transfer coefficients measured on fine wires has yielded consistently higher heat transfer coefficients than calculated from the above correlation.

5.5 Surface Effects

For the most part, heat transfer analysis for He I takes little account of the character of the surface. In steady-state heat transfer, the surface is discussed only qualitatively in terms of activated nucleation sites. Heat transfer correlations used to describe nucleate boiling and both critical heat fluxes make no attempt to include the surface character in their treatment. This clearly is a weakness in the theory for there are considerable surface-induced changes in these values. For transient heat transfer, a greater effort is put forth to include the surface physics. As was discussed in Sect. 5.6 Kapitza conductance, which is a solid-state interfacial result, must be included when attempting to understand the transient conduction heat transfer. Since surface characteristics are not generally included in engineering correlations, it is of interest to consider how variations in surface character affect experimental results.

There has not been a great deal of research conducted on surface-dependent heat transfer in He I [27–29]. In the case of steady-state investigations, surface

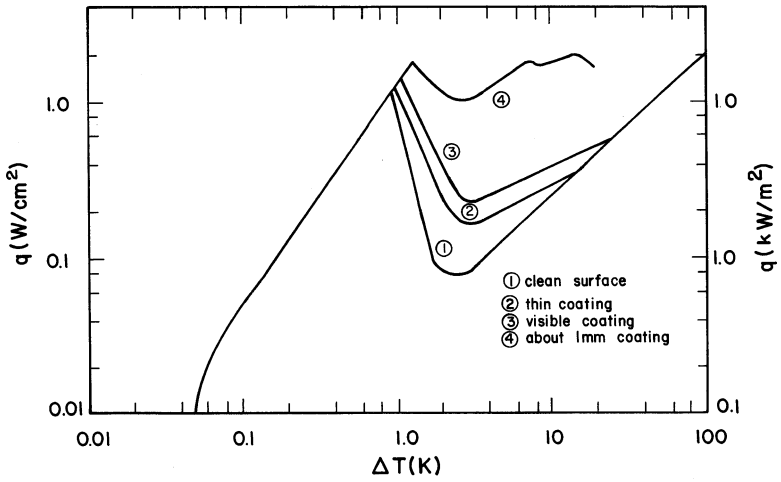

Fig. 5.16 Influence of H_2O coatings on pool boiling heat transfer (From Cummings and Smith [28])

roughness, as measured by the coarseness of the surface abrasive, strongly affects the nucleate boiling regime. This effect can be understood qualitatively by considering arguments of activated nucleation sites. The smoother the surface, the fewer active nucleation sites. Since activated sites induce convection, a polished surface should have a larger surface temperature difference ΔT_s for the same heat flux. This result has been observed by Boissin et al. [27]. Chemical treatment also has shown to affect the nucleate boiling regime [29]. These coatings combined with gross surface roughness have been employed to enhance cooling of composite conductors for large superconducting magnets.

Surface coatings also have been shown to affect the values of peak and recovery heat fluxes, q^* and q_R. The correlations used to describe these events in heat transfer do not include any of the surface characteristics. Cummings and Smith [28] have shown a clear increase in both the peak heat flux q^* and recovery value q_R with increased surface coatings. In their results shown in Fig. 5.16, the coatings were obtained by condensing H_2O crystals on the surface. Similar behavior was observed by Ogata and Nakayama [29] on chemically treated surfaces. These results are not understood in terms of heat transfer models, but they represent interesting and technically significant improvements.

5.6 Channel Heat Transfer

As a very interesting and technically significant special case of pool boiling heat transfer, consider the channel heat transfer problem described schematically in Fig. 5.17. A channel of width w is formed between a heat transfer surface and a

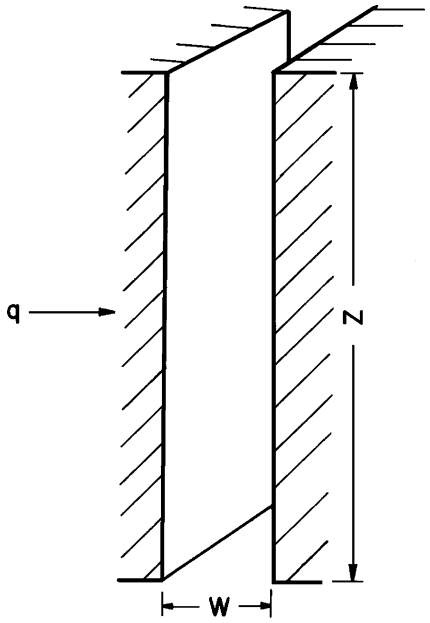

Fig. 5.17 Schematic of a heat transfer channel

second adjacent surface. The channel may be oriented at any angle between vertical and horizontal leading to variations of the heat transfer conditions. This particular problem is significant because it models an open cooling channel in a technical device such as a superconducting magnet. When heat is applied to the surface, the liquid can circulate owing to the thermosiphon effect where bubbles are transported under the influence of buoyancy forces, as discussed in Sect. 4.3.3.

If the channel is heated over its length, then the fluid accumulates vapor and the quality increases. If a low-quality fluid enters a heated tube section from below. Initially, nucleate boiling occurs at the fluid-tube interface. These bubbles are stripped from the wall and produce local bubbly flow. As the fluid continues through the tube more heat is transferred, increasing the vapor quality until slug flow and finally annular flow occur. This sequence of events is illustrated in Fig. 5.18.

Also, as the heat flux from the surface is increased, film boiling may eventually initiate at the top of the channel where the vapor quality is greatest. Because of the induced flow, the peak heat flux at the channel bottom can be quite large. The position dependence of the peak heat flux in one set of experiments is shown in Fig. 5.19. For vertically oriented surfaces in an open bath at 4.2 K, the peak heat flux is usually in the neighborhood of 6 kW/m^2. Therefore, the bottom of the channel has q^* quite close to that observed in an open bath. As the helium is vaporized and transported up the channel, the local peak heat flux is depressed. In the present example, the peak heat flux near the top approaches 3.4 kW/m^2, almost a 50% reduction.

Wilson [31] conducted one study of channel heat transfer in an experiment having variable height and width. The following set of observations were made.

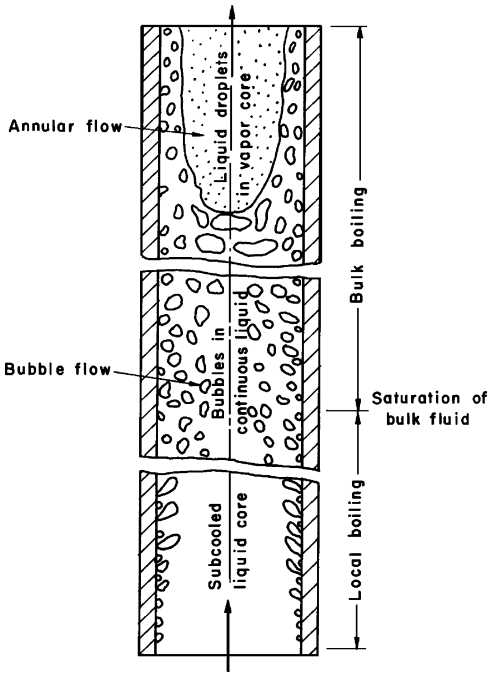

Fig. 5.18 Flow patterns in a vertical heated channel (From Tong [17])

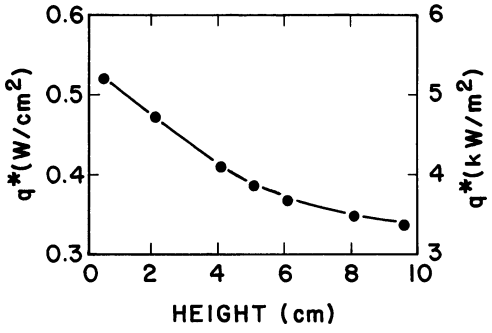

Fig. 5.19 Position dependence of the peak heat flux in a He I cooled channel (Lehangre et al. [30])

First, for small width w, the peak heat flux averaged over the entire surface area was directly proportional to the heat flux in the helium channel and therefore proportional to w. This suggests that the peak heat flux is governed by the bulk fluid flow. Second, for constant w, the peak heat flux was found to be inversely proportional to the square root of the channel height z. Based on the results as they depend on w, this indicates that the bulk heat flow varies as $z^{-1/2}$. Finally, it was found that for $w/z > 0.1$, the channel behaved effectively as an open bath with q^* approaching that of a vertically oriented surface, $q^* \sim 6$ kW/m^2.

Sydoriak and Roberts [32] derived a general relationship for frictionless homogeneous flow of a fluid in a evaporator, which Wilson applied to this channel heat

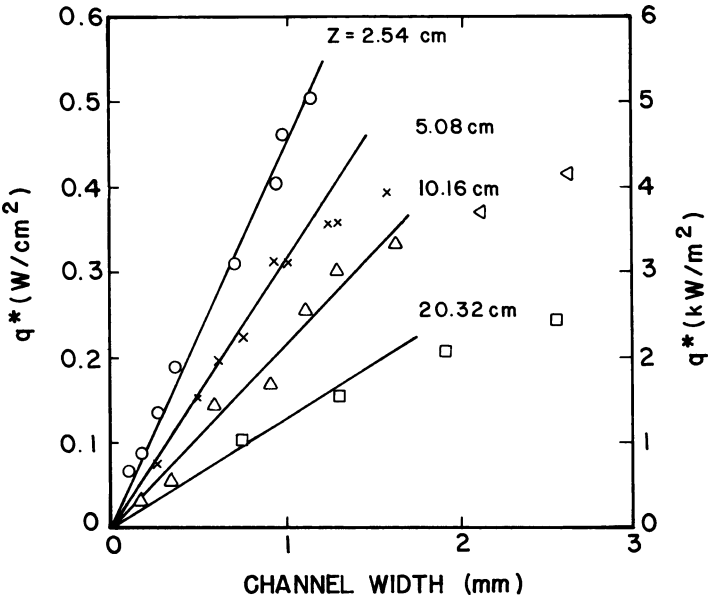

Fig. 5.20 Critical power versus channel width for He I heat transfer (From Wilson [31])

transfer problem. The prediction for the critical power per unit area of heated surface, Q^*/A_s, is given by

$$\frac{Q^*}{A_s} = \frac{w}{\sqrt{z}} \frac{h_{fg}\rho_l}{2} \left[\frac{g\tilde{q}}{\beta - 1} \left(1 - \frac{\ln[1 + \tilde{q}(\beta - 1)]}{\tilde{q}(\beta - 1)} \right) \right]^{1/2} \tag{5.35}$$

where $\beta = \rho_l/\rho_v$ and $\tilde{q}$ is the "critical quality" – the mass ratio of vapor to total (liquid plus vapor) at the channel top when film boiling initiates. This last quantity must be determined empirically although in general it should be a scalable function for different fluids.

A plot of the critical power versus channel width w for different channel lengths z should give a linear plot from which the proportionality function $Q^* z^{1/2}/wA_s$ can be determined. Such a plot is displayed in Fig. 5.20 for four different channel heights. The linear plot obtained yields a critical quality $\tilde{q}$ ranging from 0.33 to 0.26 in the case of the largest channel. Thus, for calculations, (5.35) should be a reasonable approximation for Q^*/A_s assuming a constant value for $\tilde{q} \approx 0.3$.

One difficulty with the above described analysis is that it does not naturally lead into the open bath limit for $w/z > 0.1$. In an effort to develop a more general equation for channel heat transfer, Lehangre et al. [30] suggested a correlation based on a series of experiments of different configuration:

$$\frac{Q^*}{A_s} = \frac{10}{1.7 + 0.125(z/D_h)^{0.88}} \tag{5.36}$$

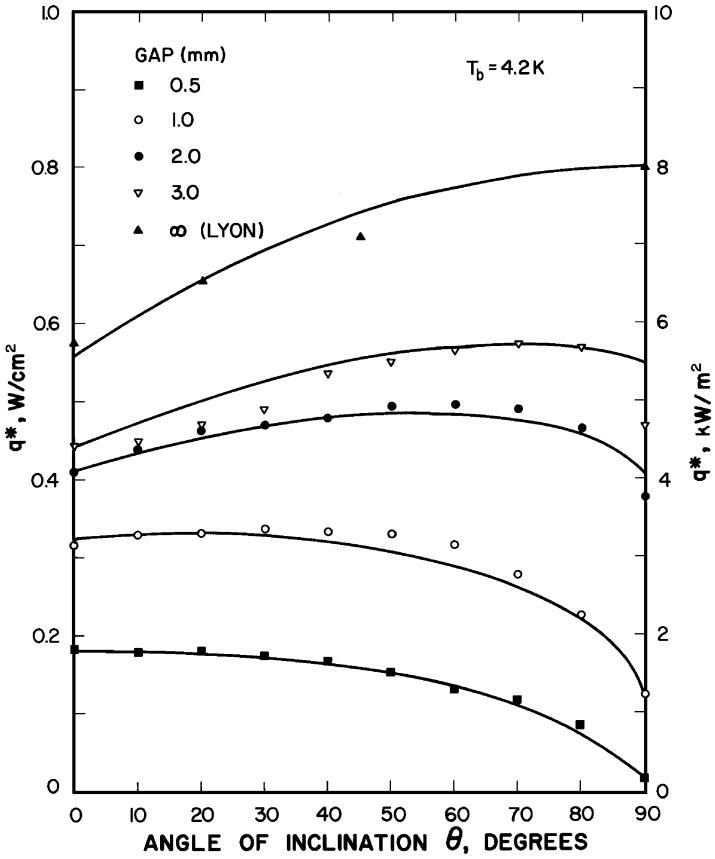

Fig. 5.21 Variation of the peak heat flux with channel orientation and width at 4.2 K. Channel is 127 mm in length [33]

where Q^*/A_s is in kW/m^2. The quantity D_h is the hydraulic diameter which is equal to four times the ratio of the flow cross section to the heated perimeter. Equation (5.36) has the appropriate limit for w/z large; however, for channels other than in the vertical orientation it is not applicable.

Chen and Van Sciver [33] noted that for wide channels the maximum heat flux q^* should correlate with the open bath pool boiling results by Lyon [20] (see Fig. 5.11). The results of these experiments are shown in Fig. 5.21, where the angle θ is measured from the vertical orientation. There are two physical processes that lead to the observed angular dependence of q^*. The first process is nucleate boiling associated with movement of vapor bubbles normal to the heated surface. This effect, which is maximum at an angle of 90°, can be assumed to control the heat transfer process for large w. The other process is associated with the natural circulation of the heated fluid, where the movement is parallel to the heated surface. The natural circulation process is a maximum at $\theta = 0°$ and should

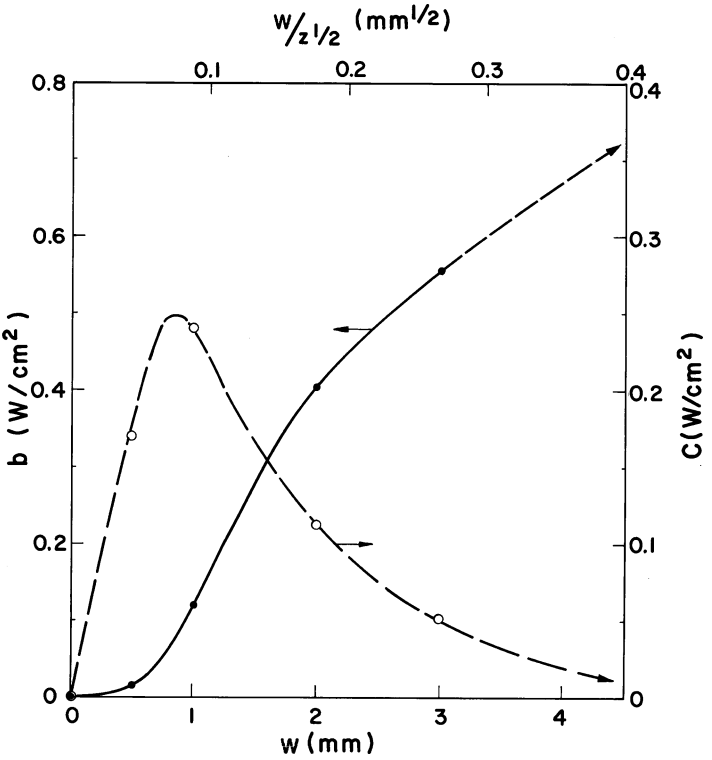

Fig. 5.22 Parameters used to fit the variation of q^* with θ in (5.37)

dominate the heat transfer in the limit of small w. The combination of these two processes is necessary to describe the variation of q^* with θ and w. In particular, one would expect the maximum value of q^* to vary continuously between 0° and 90° as the channel width is increased.

A general correlation used to describe the angle and width dependencies of q^* is of the form

$$q* = b \ \sin\left(\frac{\theta + 90^\circ}{2}\right) + c(\cos\theta)^{1/2} \tag{5.37}$$

where b and c are adjustable parameters, which should be functions of w only. The width dependence of these parameters is shown in Fig. 5.22. The basis for (5.37) is purely empirical evidence. The first term is used to describe the nucleate boiling heat transfer process. The angular dependence is in reasonable agreement with Lyon's pool boiling data. The second term represents the natural circulation process. The $(\cos\theta)^{1/2}$ angular dependence not only fits the experimental data for small w but is consistent with the Wilson's correlation which predicts $q^* \propto g^{1/2}$.

As a final comment on channel heat transfer, the steady-state conditions as described above generally take a considerable time to become established. This is because the natural circulation requires a substantial temperature rise and vapor production before it is fully established. Naturally, the time to reach steady state depends on the magnitude of Q^*/A_s, but for significant heat fluxes, of the order of 1 kW/m^2, this characteristic time can be as much as a second. The existence of a characteristic time for the development of steady-state heat transfer has strong impact on technical applications. Since many systems experience transient heat transfer processes, which are on the millisecond time scale, it is important to appreciate that these heat transfer processes are far from steady state.

5.7 Forced Convection Heat Transfer

The process of heat transfer to forced flow helium is closely tied to the dynamics of the flow states, a topic covered in Sect. 4.1. In the present section, we would like to extend that discussion to include solutions to the energy equation that can be used to treat convective transfer.

5.7.1 General Considerations

The problem of interest involves heat transfer from a surface exposed to flowing liquid helium. If the predominant flow is in the x-direction and the heat transfer is in the direction perpendicular to that of the flow (y-direction), the energy equation may be simplified by using the thermal boundary layer approximation,

$$\frac{\partial T}{\partial y} \gg \frac{\partial T}{\partial x}$$

which is analogous to that assumed for the velocity profile. Assuming for simplicity that the fluid possesses constant properties ρ, C_p, k, and μ, we obtain the corresponding thermal boundary layer equation [2],

$$u\frac{\partial T}{\partial x} + v\frac{\partial T}{\partial y} = \alpha\frac{\partial^2 T}{\partial y^2} + \frac{\mu}{\rho C_p}\left(\frac{\partial u}{\partial y}\right)^2 \tag{5.38}$$

where $\alpha = k/\rho C_p$ is the thermal diffusivity. The first term on the right-hand side of (5.38) represents thermal diffusion. For most fluids of interest in cryogenics, this term is not large and can be neglected.

By suitable normalization, (5.38) can be shown to lead to the definition of the Nusselt number as a general function of Reynolds number and Prandtl number, that is,

$$Nu = \mathrm{f}(\mathrm{Re}_D, \mathrm{Pr}) \tag{5.39}$$

For internal flow, the Nusselt number is defined as:

$$Nu_{D_h} = \frac{hD_h}{k_f} \tag{5.40}$$

where k is a suitably averaged fluid thermal conductivity. In fact, (5.40) is general and not dependent on the boundary layer approximation. Most empirical heat transfer correlations are constructed in a form consistent with (5.39).

5.7.2 Heat Transfer Correlations

Investigations of heat transfer to forced convection helium have shown that traditional engineering correlations are best at describing the data. Results of analysis of the thermal boundary layer indicate that the average Nusselt number should be couched in a form consistent with (5.39). As an aside, be aware that the local heat transfer coefficient can be a considerable function of temperature and therefore varies along the length of the tube. The local heat transfer coefficient is also defined in terms of the local mean fluid temperature,

$$h = \frac{q}{T_s - T_m} \tag{5.41}$$

where T_m is obtained by taking an appropriate average across the channel.

There are numerous single-phase fluid heat transfer correlations for internal flow. Several important factors must be considered when selecting a correlation to apply to a particular system. First, determine whether the fluid is in the laminar or turbulent flow regime. The critical Reynolds number for single-phase internal flow is around 1,200. Second, determine whether the entry region has significant impact on either the hydrodynamics or temperature development. This requirement demands fairly large L/D ratios. Helium has a Prandtl number of the order of unity, so it is expected that these developments will occur almost simultaneously. Finally, once the conditions of flow are established, it is necessary to select among several possible correlations dependent on whether the range of parameters is appropriate for the particular empirical fit.

In fully developed laminar internal flow, there are analytic solutions to the thermal boundary layer equations of the form,

$$Nu_D = \text{constant} \tag{5.42}$$

Where the constant depends on boundary conditions being 4.36 for constant heat flux boundary conditions and 3.66 for constant wall temperature boundary conditions. However, for most helium cryogenic problems, laminar flow almost never occurs. One exception involves flow within porous media a topic discussed below.

For turbulent flows, all engineering correlations are of the form of (5.39) where the average Nusselt number is a function of the fluid Reynolds and Prandtl numbers. In this regime, a number of good correlations exist for single-phase turbulent heat transfer. The Dittos–Boelter expression is perhaps the most common such heat transfer correlation [2],

$$\overline{\mathrm{Nu}} = 0.023 \mathrm{Re}_D^{4/5} \mathrm{Pr}^{2/5} \tag{5.43}$$

where $\overline{\mathrm{Nu}}$ represents the average Nusselt number over the tube length. Correct application of this expression demands consideration of the temperature dependence of the fluid properties. The appropriate properties must be evaluated at the film temperature T_f, defined by

$$T_f = \frac{T_s + T_m}{2} \tag{5.44}$$

which is a simple average between the surface and mean fluid temperatures. The Dittus-Boelter correlation has been used quite effectively for a variety of cryogenic heat transfer problems [34].

In the case of supercritical helium, Giarratano et al. [35] have suggested that a prefactor of 0.022 gives a better fit to their data with a standard deviation of

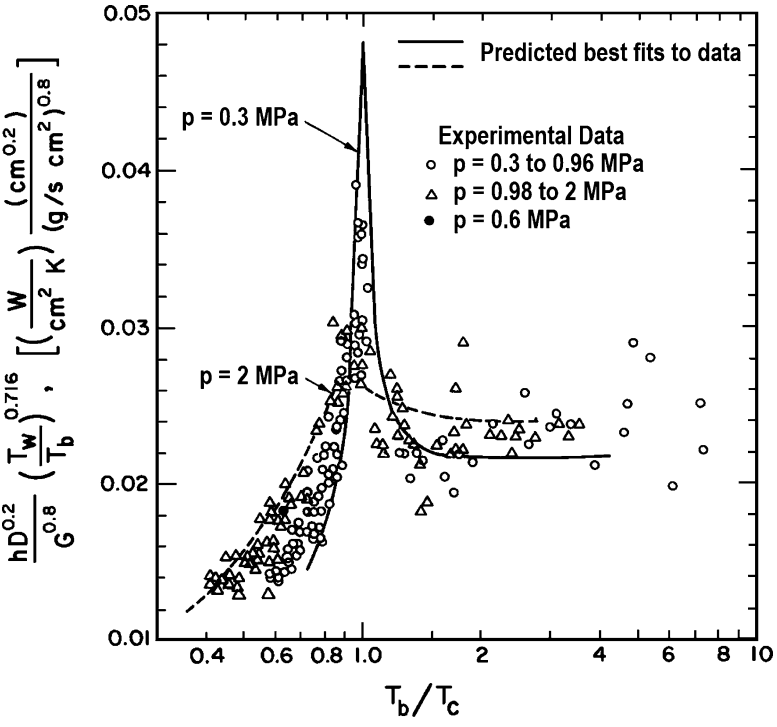

Fig. 5.23 Experimental and predicted heat transfer results for supercritical helium using (5.45) (From Giarratano et al. [35])

14.8% obtained between experimental results and correlation. An improved fit to the experimental data was achieved by use of a slightly modified correlation of the form [13]

$$\mathrm{Nu} = 0.0259\ \mathrm{Re}_D^{4/5}\mathrm{Pr}^{2/5}\left(\frac{T_s}{T_m}\right)^{-0.716} \tag{5.45}$$

where now explicit temperature variation of the properties is taken into account by the last factor. The relationship given by (5.45) correlated to a standard deviation of 8.3% with several sources of experimental data. A normalized form of this comparison is shown in Fig. 5.23, where the heat transfer coefficient is plotted against reduced temperature T_b/T_c, where T_c is the critical temperature.

In general, heat transfer to fully developed forced flow single phase helium can be assumed to have a well-established engineering basis. Since the fluid is single phase, its hydrodynamics can be evaluated in terms of the Navier–Stokes equation of motion including compressibility factors. This problem is quite difficult owing to the variability of physical properties with pressure and temperature. Consequently, its solution requires numerical integration of complicated nonlinear equations. Be aware that this particular problem represents only one special case of forced flow helium. Other problems concerning two-phase flow and transient effects, subjects of subsequent sections in this chapter, are more complex in physical nature.

Example 5.2

Consider a thin walled copper tube of diameter 10 mm carrying liquid helium at 1 g/s and subject to a surface heat flux of 0.1 kW/m^2. The helium enters the tube at 4.2 K and 0.2 MPa. Calculate the tube wall temperature.

At the given temperature and pressure, the properties of helium are: $\rho = 125$ kg/m^3; $\mu = 3 \times 10^{-6}$ Pa s; $k_f = 0.018$ W/m K; Pr = 0.792
For the given flow conditions, the Reynolds number is,

$$\mathrm{Re}_D = \frac{\rho u D}{\mu} = \frac{4\dot{m}}{\pi \mu D} = 42,441$$

Using the Dittus Boelter correlation,

$$\overline{\mathrm{Nu}} = 0.023\,\mathrm{Re}_D^{4/5}\mathrm{Pr}^{2/5} = 105$$

And the heat transfer coefficient,

$$h = \frac{Nu * k_f}{D} = 190\,\mathrm{W/m^2\,K}$$

For a surface heat flux of 1 kW/m^2, this means that the tube surface is 0.526 K above that of the fluid or 4.726 K.

5.7.3 Two Phase Flow Heat Transfer

Two-phase flow in subcritical helium is a complex problem as was discussed in section 4.3; however, the difficulty in understanding the processes involved in two phase flow increases significantly when heat transfer is included. In addition to mass flow rate, vapor quality, and void fraction determining the flow conditions, the effect of heat flux into the fluid also must be considered. In particular, heat transfer can lead to rapid variations of vapor quality along the tube section.

Experimental investigations of two-phase flow heat transfer have been carried out by de La Harpe et al. [36] and Johannes [37]. These studies consist principally of forced flow helium at 4.2 K confined to a tube of a few mm ID with temperature and pressure probes necessary to determine the heat transfer coefficient and critical heat flux for boiling. The latter quantity is strongly geometry dependent and cannot be generalized easily in other systems.

The heat transfer coefficient obtained for two-phase helium is discussed best in terms of classical correlating relationships. The approach is to determine first the Nusselt number corresponding to the Dittus–Boelter equation for the liquid flow only, that is,

$$\mathrm{Nu}_l = 0.023(\mathrm{Re}_l)^{0.8}(\mathrm{Pr}_l)^{0.4}(1-\chi)^{0.8} \tag{5.46}$$

where the last multiplier is to indicate the contribution of only the liquid. Note that $\mathrm{Nu}_l = hD_h/k_l$, where k_l is the liquid thermal conductivity. Measurements of the two-phase heat transfer coefficient have shown that the actual Nusselt number normalized to (5.46) can be correlated to the Lockhart–Martinelli parameter, χ_{tt}, as

$$\frac{Nu_{\exp}}{Nu_l} = A\chi_{tt}^{-n} \tag{5.47}$$

where χ_{tt} is discussed in Chap. 4 and repeated here for convenience,

$$\chi_{tt}^2 = \frac{(dp/dx)_v}{(dp/dx)_l} \tag{4.37}$$

The best fit to the data of Johannes [37] of the form of (5.47) are displayed in Fig. 5.24 for which the appropriate values are $A = 5.40$ and $n = 0.385$. Results of de La Harpe [36] are also displayed as the dashed line in the figure with agreement in form to the data of Johannes, although possessing substantially different values for the coefficient A. Although the above correlation seems appropriate for low to

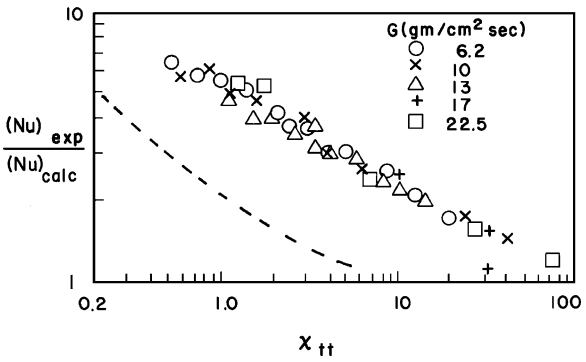

Fig. 5.24 Two-phase heat transfer correlation for helium (From Johannes [37]). The *dashed line* is a comparison to previous measurements of de La Harpe et al. [36]

moderate values of the Lockhart–Martinelli parameter, in the limit of large χ_{tt}, which occurs for small vapor quality, the ratio given by (5.47) must approach unity. Therefore, to be universally applicable the correlation should reflect this fact.

Two-phase heat transfer as with two-phase flow is a complex process which is very difficult to understand fully. If faced with a problem in this area, the best approach is to apply one of the accepted correlations. However, these calculations are only approximate and should be used only as a guide. If greater accuracy is required, experimental modeling is the required approach.

5.8 Transient Heat Transfer

In the previous sections, it was assumed that the heat transfer process had been underway for sufficient time that steady-state conditions existed. The characteristic time required for the steady state to be achieved is equivalent to the time required for convection to become fully established. For nucleate boiling, enough heat must be transferred to vaporize bubbles and allow them to detach. In film boiling the characteristic time is associated with sufficient energy flux to vaporize a layer of helium. This can be represented approximately by

$$\Delta t \approx \frac{\rho h_{fg} \delta}{q} \tag{5.48}$$

where δ is the vapor film thickness. For an order-of-magnitude analysis assume that $\delta \approx 10$ μm. Using the physical quantities for He I at 4.2 K, 0.1 MPa, (5.48) predicts $\Delta t \approx 3/q$ ms, where q is in W/cm^2. For a heat flux of a few W/cm^2, the steady-state conditions are not established until well in excess of a few milliseconds. For times shorter than this value, the heat transfer processes are governed by nonconvective mechanisms such as conduction and radiation.

It is of considerable importance to be able to understand transient heat transfer in liquid helium. Transient heat transfer is fundamental to the analysis of a number of problems including the stability of superconducting magnets. There are several

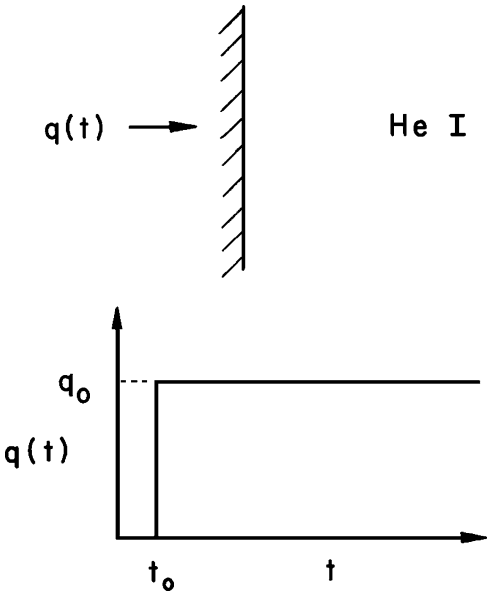

Fig. 5.25 Schematic representation of the transient heat transfer process

aspects to this problem which are worth noting at the beginning. First, for very short times, that is, $\Delta t < 1$ ms, heat transfer processes turn out to be controlled by physical mechanisms similar to those developed for the case of He II, that is, Kapitza conductance. Second, the transition between the region of heat transfer space governed by conduction and that which resembles the steady-state process is important. This transition occurs on time scales consistent with the rough calculation in above. There are several parameters that are associated with transient heat transfer. (1) the peak heat flux $q^*(t)$ or critical energy $\Delta E^* = q^* \Delta t^*$; (2) the interfacial temperature difference ΔT_s; and (3) the effective heat transfer coefficient h. These parameters are governed primarily by the physical properties of helium and the rate of heat transfer.

The various regimes of transient heat transfer can be described best in terms of an idealized experiment, which in fact is not very different from actual experiments performed to investigate the problem. Imagine a solid heat transfer surface as shown in Fig. 5.25, which in this particular case is oriented vertically. Recall that the peak steady-state heat flux for this configuration is in the neighborhood of 6 kW/m^2. In this experimental configuration, a step function heat flux q_0 beginning at t_0 is applied to the sample. With suitable thermometry, which must have a response time faster than a millisecond, the surface temperature is recorded as it varies with time following the initiation of heat transfer.

As an example of the kind of data collected from this type of experiment, measurements by Steward [38] are shown in Fig. 5.26. In this particular case, the heat transfer surface is a thin carbon film which is both heater and thermometer.

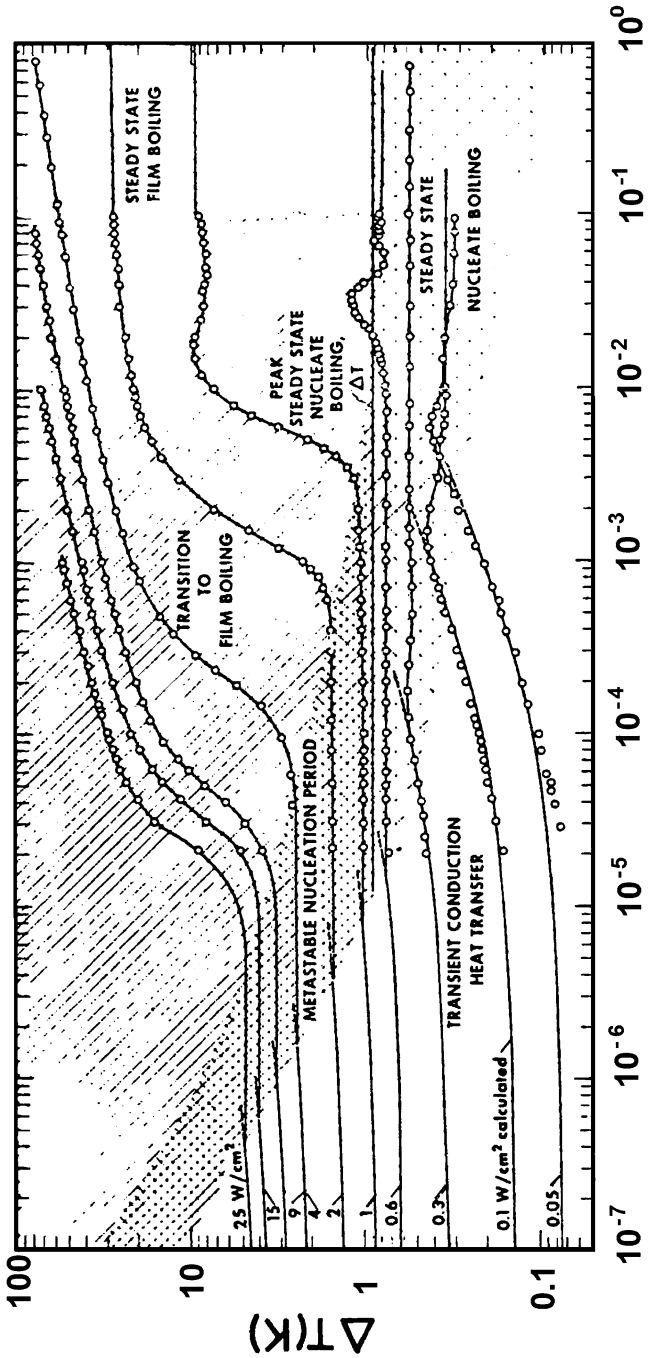

Fig. 5.26 Transient heat transfer to saturated liquid He I from a vertically oriented heater (From Steward [38])

Note that for very short times, the surface temperature rise is not large, although it is an increasing function of heat flux. This short time regime, which is generally much less than 1 ms, is controlled by transient conduction mechanisms. As time progresses, the nucleation of convective mechanisms begins. For low heat fluxes, the heat transfer process eventually transforms to steady-state nucleate boiling. At high heat fluxes, that is, $q > 10$ kW/m^2 (1 W/cm^2), there is a transition to the film boiling state. This latter transition has associated with it an increase in ΔT_s of about an order of magnitude, consistent with the steady-state film boiling heat transfer characteristics. In the steady-state regime, the temperature differences presumably can be described in terms of the correlations introduced in previous sections of this chapter. There are, however, two effects in these data which need further discussion: (1) the size of the heat transfer coefficient in the transient conduction regime and (2) the time associated with the transition to steady-state heat transfer mechanisms.

5.8.1 Surface Temperature Difference

Consider first the problem of the surface temperature difference during transient conduction. Since this mechanism is conduction dominated, it should be possible to understand in terms of diffusion theory. Returning to Fig. 5.25, imagine a steady heat flux through the interface. There are two potential contributors to the associated temperature difference. First, there is a thin fluid layer of thickness δ into which the heat diffuses. The temperature difference across the layer, defined as ΔT_f, should be determined exclusively by heat diffusion in the bulk fluid. Second, there is an interfacial temperature difference that is due to the mismatch of phonon heat transport between the two media. This mechanism, referred to as Kapitza conductance, which will be discussed in Chap. 7. It is a truly interfacial process occurring within a few atomic layers of the solid-helium boundary. The temperature difference due to Kapitza conductance is given the designation ΔT_k.

To evaluate the heat diffusion temperature difference, it is necessary to solve the heat diffusion equation with the proper set of boundary conditions. In one dimension this equation can be written

$$\frac{\partial^2 \Delta T_f}{\partial x^2} = \frac{1}{D}\frac{\partial \Delta T_f}{\partial t} \tag{5.49}$$

given a number of simplifying assumptions. In particular, it is assumed that the thermal diffusivity, $D = k/\rho C$, is a constant independent of temperature or position. Of course, this is not a particularly good assumption for liquid helium, however, it simplifies the model considerably to do so. Furthermore, it is assumed that the solid does not play a major role in the heat diffusion. This approximation has a negligible

effect if the heat transfer surface has small heat capacity. The boundary conditions which are applied to solve (5.49) include

$$\Delta T_f(x,0) = 0 \tag{5.50a}$$

$$\Delta T_f(\infty,t) = 0 \tag{5.50b}$$

and

$$q = -k\frac{\partial \Delta T_f}{\partial x}\bigg|_{x=0} \tag{5.50c}$$

The last condition, being consistent with the constant flux assumption at the interface, is true only if the heat capacity of the heat transfer surface is neglected. The general solution to (5.49) with the above set of boundary conditions leads to

$$\Delta T_f = \frac{q}{k}\left[2\left(\frac{Dt}{\pi}\right)^{1/2}\exp\left(\frac{-x^2}{4\,Dt}\right) - x\ \mathrm{erfc}\left(\frac{x}{2(Dt)^{1/2}}\right)\right] \tag{5.51}$$

where x is the dimension measured into the fluid. At the solid-fluid interface, x $= 0$, the relationship simplifies considerably to yield

$$\Delta T_f = \frac{2q}{\sqrt{\pi}}\left(\frac{t}{\rho k C}\right)^{1/2} \tag{5.52}$$

For example, consider liquid helium at 4.2 K subjected to a heat flux of 1 W/cm^2 for a time of 10 μs, which is in the transient conduction regime. These conditions lead to a computed value for ΔT_f of about 0.3 K, which is approximately equal to the superheat required to produce homogeneous nucleation computed in Sect. 5.3. It is also worth noting that $\Delta T_f \approx 0.3$ K corresponds to about 1/3 the measured ΔT in Fig. 5.26.

The second mechanism which can lead to an interfacial temperature difference during transient heat transfer is due to Kapitza conductance. The temperature dependence of the Kapitza conductance is understood but the absolute value of the heat transfer coefficient is not predictable. Assuming. that the mechanisms are the same independent of whether the fluid is He I or He II, it is reasonable to write

$$\Delta T_K \simeq \frac{q}{h_K} \tag{5.53a}$$

where $h_K \simeq AT^3$, consistent with experimental measurements of Kapitza conductance. For a copper surface below T_λ, A has been measured to have values around 0.1 W/cm^2·K^4, but with considerable uncertainty. Using this value for $T_b = 4.2$ K in He I, the interfacial temperature difference due to Kapitza conductance should

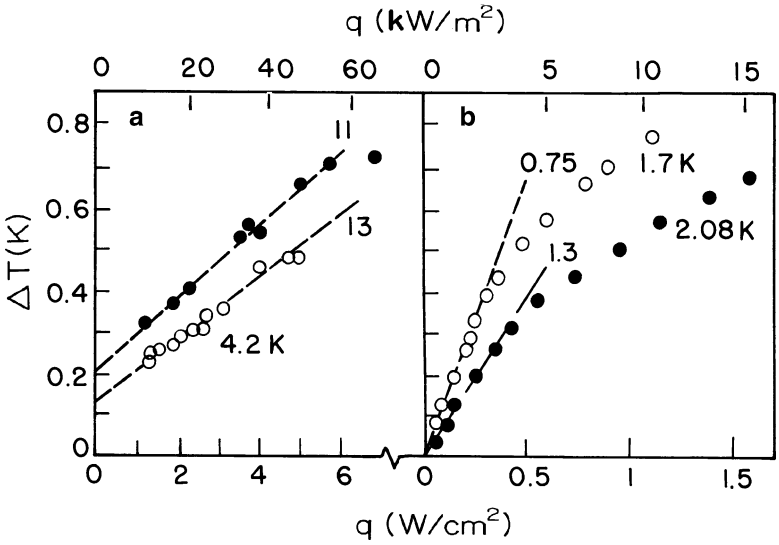

Fig. 5.27 Surface temperature difference for copper samples versus heat flux: (**a**) He I at 4.2 K and (**b**) He II at 1.8 K. Numbers on the straight lines refer to h values in W/cm·K (From Schmidt [39])

vary as $\Delta T_K \approx 0.13\ q$. Therefore, for copper, the Kapitza temperature difference would be the same order as but somewhat smaller than that due to transient conduction except at very short times, $t \lesssim 1\ \mu$s.

On a very short time scale the heat flux dependence of the heat transfer coefficient in He I generally obeys the processes described above. Plotted in Fig. 5.27 is the surface temperature difference for copper samples measured in He I compared to that for He II [39]. On the right-hand side, the figure shows a typical ΔT_s versus q dependence observed for He II. Initially, there is a linear region; however, as the heat flux increases a considerable deviation from linearity occurs because the actual heat transfer varies as $T_s^n - T_b^n$ where $n \approx 3$. A somewhat different effect is observed for the case of He I. Here the dependence of ΔT versus q for high heat fluxes is almost linear, indicating a constant heat transfer coefficient. However, at low heat fluxes the surface temperature does not appear to extrapolate to the origin, indicating some failure in the linear modeling over the regime for which the linear relationship holds. The Kapitza conductance appears to obey the cubic temperature dependence.

In principle, the temperature difference corresponding to a transient heat transfer event can be determined by a series summation of the two contributions described above. It follows that

$$\Delta T_s = \Delta T_K + \Delta T_f \tag{5.53b}$$

where, dependent on the choice of surface materials, one term can dominate the process. For comparison with theory, it should be possible to separate the two quantities in (5.53b) based on their different time dependencies.

5.8.2 Transition to Film Boiling

The other fundamental question related to transient heat transfer concerns the onset of film boiling. For a given heat flux q^*, the time required to reach the film boiling state, Δt^*, is of interest. This quantity establishes the limits to which enhanced heat transfer due to transient conduction can be credited in a heat transfer problem. The problem is understandable by means of a rather simple picture. Given that the transition is associated with the formation of a vapor film, a critical energy is defined as that required to vaporize the helium adjacent to the heat transfer surface and create the film.

A more quantitative model can be developed by assuming that ΔE^* is the energy needed to vaporize a layer of thickness δ, which corresponds to the diffusion length. Employing the transient diffusion model, we note that the diffusion length can be approximated by

$$\delta = \frac{\pi}{2}(Dt)^{1/2} \tag{5.54}$$

where again D is the thermal diffusivity. On a unit area basis, the critical energy is written

$$\Delta E^* = q^* \Delta t^* = \delta h_{fg} \tag{5.55}$$

where h_{fg} is the heat of vaporization of liquid helium at the existing temperature and pressure conditions. Substituting (5.54) into (5.55), we find that the heat flux needed to achieve film boiling is given by

$$q^* = \frac{\pi}{2}\rho h_{fg}\left(\frac{k}{\rho C\ \Delta t^*}\right)^{1/2} \tag{5.56}$$

which for values associated with He I at 4.2 K, 1 bar, simplifies to

$$q^* = 0.07\left(\Delta t^*\right)^{-1/2} \tag{5.57}$$

where q^* is in W/cm^2 and Δt^* is in seconds. Note that this correlating equation does not contain any adjustable parameters. Plotted in Fig. 5.28 are numerous experimentally determined values for q^* along with the simple diffusion model fit given by (5.57). The correspondence is surprisingly good, which supports the basic physical ingredients to the critical energy analysis included in the simple model. A more precise empirical fit has been suggested [39]:

$$q* = 0.127\left(\Delta t^*\right)^{-0.4} \tag{5.58}$$

This form is seen to agree with the data, particularly in the sub-millisecond regime.

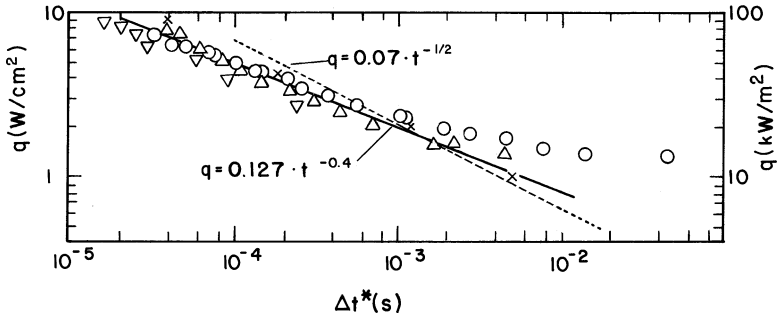

Fig. 5.28 Heat flux versus time for transition to film boiling (As compiled by Schmidt [39])

As a final comment, the transient heat transfer analysis given above is oversimplified. Only two problems have been discussed, the heat transfer coefficient in the conduction regime and the critical energy for the onset of film boiling. In between these two regimes is the transition to film boiling including the dynamics of nucleation and the creation of the vapor film. These are considerably more complex phenomena than can be discussed here. This regime has been analyzed to some extent by Steward [38] by evaluating the orientation and pressure dependence to the type of data displayed in Fig. 5.26. The observations gleaned from this work are more qualitative but suggest that the transition regime is at least in part controlled by conventional heat transfer phenomena. Further work is required to grasp more fully the various aspects of the transient heat transfer problem.

Questions

1. For pool boiling liquids, why is the heat transfer coefficient in nucleate boiling higher than the heat transfer coefficient in free convection?
2. In pool boiling heat transfer, q* depends on surface orientation. Discuss in terms of the bubble formation and detachment picture, why surface orientation should make a difference and what would be the expected trend. $q^* > 0$ in pool boiling heat transfer even for the face down condition, $\Theta = 180$. Why?
3. Discuss the trends in the He I nucleate boiling curve (Fig. 5.9). Is there any correlation with surface roughness? If so, how would this trend be explained in terms of bubble nucleation theory?

Problems

1. Calculate the critical radius of a vapor nucleus in He I at 4.2 and 2.5 K under saturated vapor pressure. Assume a reaction rate of 1 $cm^{-3} \cdot s^{-1}$. Compare this value with the radius determined from (5.15). Estimate the reaction rate consistent with the radius determined from (5.15).

2. Determine the surface temperature at which the maximum in the peak nucleate boiling heat flux q^* in saturated He I occurs. What would be the change in this value if the system we pressurized to $p = 200$ kPa?
3. A vertically oriented, circular cross section channel containing He I at 4.2 K is exposed to a heat flux which varies linearly with height:

$$Q(z) = Q_m\left(\frac{z}{H}\right)$$

where H is the total channel height. Determine as a function *of* Q_m the position where the peak heat flux is first exceeded.
4. The Schmidt model for the transition to film boiling during transient heat transfer, (5.56), implies that the transition occurs when the surface reaches a temperature that is a constant for a given helium bath. Find an expression for the critical surface temperature in the Schmidt model and calculate its value for a saturated He I bath at 4.2 K. Compare your answer with the homogeneous nucleation temperature for the same conditions.
5. Consider film boiling heat transfer from a flat plate in He I. Calculate the plate surface temperature at the minimum film boiling heat flux q_R.
6. A heat exchanger cools supercritical helium at 1 MPa from 6 to 4.5 K. The design consists of a tube immersed in the saturated bath of He I at 4.2 K. Determine the length and diameter of the tube consistent with the following specification: $\dot{m} = 1$ g/s and $\Delta p = 0.01$ MPa . For simplicity assume isothermal conditions on the external surface of the tube.
7. A pool boiling cooled superconducting magnet uses a monolithic conductor 30 mm wide and 3 mm thick. The conductor is cooled on one face by liquid helium in the gap between adjacent turns of 0.5 mm. Calculate the peak heat flux for this conductor in helium at T = 4.6 K, 0.14 MPa, if the wide surface is vertical. How would this result change if the conductor were exposed to an open bath of liquid helium instead of a narrow channel?

References

1. See for example, E. R. G. Eckert and R. M. Drake, *Analysis of Heat and Mass Transfer*, McGraw–Hill, New York, 1972.
2. See for example, F. P. Incropera and D. P. Dewitt, *Fundamentals of Heat Transfer*, Wiley, New York, 1981.
3. J. A. Whitehead, *Survey of Hydrodynamic Instabilities, in Fluctuations, Instabilities and Phase Transitions*, Tormad Riste (Ed.), pp. 153–180, Plenum Press, New York, 1975.
4. R P. Behringer and G. Ahlers, Heat Transport and Temporal Evolution of Fluid Flow Near the Rayleigh-Bénard Instability in Cylindrical Containers, *J. Fluid Mech.* **125**, 219 (1982).
5. F. Irie, G. Kippling, K. Uders, T. Matsushita, U. Ruppert, and M. Takeo, Heat Transfer to Helium in the Near Critical Region, *Adv. Cryog. Eng.* **23**, 326 (1978).
6. M. A. Hilal, R. W. Boom, and M. M. El-Wakil, An Experimental Investigation of Free Convection Heat Transfer in Supercritical Helium, *Int. J. Heat Mass Transfer* **23**, 697 (1980).

7. G. Kippling and K. Kutzner, in *Pure and Applied Cryogenics*, **Vol. 6**, pp. 97–107, Pergamon Press, Oxford, 1967.
8. M. A. Hilal, Analytical Study of Laminar Free Convection Heat Transfer to Supercritical Helium, *Cryogenics* **18**, 545 (1978).
9. D. N. Sinha, J. S. Semura, and L. C. Brodie, Homogeneous Nucleation in 4He: A Corresponding States Analysis, *Phys. Rev.* **A 26**, 1048 (1982).
10. J. Frenkel, *Kinetic Theory of Liquids*, Chap. 7, Dover, New York, 1955.
11. E. Flint and J. Van Cleve, Heat Transport to He I from Polished Silicon Surface, *Adv. Cryog. Eng.* **27**, 283 (1982).
12. Y. Y. Hsu and R. W. Graham, An Analytical and Experimental Study of the Thermal Boundary Layer and the Ebullition Cycle in Nucleate Boiling, *NASA TN D-594* (1961).
13. W. B. Bald, Cryogenic Heat Transfer Research at Oxford, Part I, Nucleate Pool Boiling, *Cryogenics* **13**, 457 (1973).
14. S. S. Kutateladze, *Statistical Science & Technical Publications of Literature on Machinery*, Atomic Energy Commission Translation 3770, Technical Information Services, Oak Ridge, TN (1949), 1952.
15. W. B. Bald and T. V. Wang, The Nucleate Pool Boiling Dilemma, *Cryogenics* **16**, 314 (1976).
16. C. Schmidt, Review of Steady State and Transient Heat Transfer in Pool Boiling Helium I, in *Stability of Superconductors*, pp. 17–32, International Institute of Refrigeration Commission A 1/2, Saclay, France, 1981.
17. L. S. Tong, *Boiling Heat Transfer and Two Phase Flow*, Chap. 2, Wiley, New York, 1965.
18. N. Zuber, M. Tribes, and J. W. Westwater, The Hydrodynamic Crisis in Pool Boiling of Saturated and Subcooled Liquids, in *International Development in Heat Transfer*, Part. II, pp. 230–234, ASME, New York, 1961.
19. R. V. Smith, Review of Heat Transfer to Helium I, *Cryogenics* **9**, 11 (1969).
20. D. N. Lyon, Boiling Heat Transfer and Peak Nucleate Boiling Fluxes in Saturated Liquid Helium Between λ and Critical Temperatures, *Adv. Cryog. Eng.* **10**, 371 (1965).
21. E. Ibrahim, R. W. Boom, and G. E. McIntosh, Heat Transfer to Subcooled Liquid Helium, *Adv. Cryog. Eng.* **23**, 333 (1978).
22. R. Capri, Heat Transfer to Subcooled He I, *Adv. Cryog. Eng.* **29**, 281 (1984).
23. Yu. Kirichenko, K. V. Rusanov, and E. G. Tyurina, Heat Transfer in Subcooled Liquid Cryogens, *Cryogenics* **23**, 209 (1983).
24. J. H. Lienhard and P. T. Y. Wong, The Dominant Unstable Wavelength and Minimum Heat Flux During Film Boiling on a Horizontal Cylinder, *J. Hear Transfer* **86**, 220 (1964).
25. B. P. Breen and J. W. Westwater, Effects of Diameter of Horizontal Tubes on Film Boiling Heat Transfer, *Chem. Eng. Prog.* **58**, 67 (1962).
26. E. G. Brentari, P. J. Giarratano, and R. V. Smith, Boiling Heat Transfer for Oxygen, Nitrogen, Hydrogen, and Helium, *NBS Technical Note 317*, U.S. Government Printing Office, Washington, DC, Sept. 20, 1965.
27. J. C. Boissin, J. J. Thibault, J. Roussel, and E. Faddi, Boiling Heat Transfer and Peak Nucleate Boiling Flux in Liquid Helium, *Adv. Cryog. Eng.* **13**, 607 (1967).
28. R. D. Cummings and J. L. Smith, Boiling Heat Transfer to Liquid Helium, Liquid Helium Technology, *Proceedings of the International Institute of Refrigeration*, Commission 1, Boulder, CO, Pergamon Press, Oxford, 1966, pp. 85–96.
29. H. Ogata and W. Nakayama, Boiling Heat Transfer to Helium from Machined and Chemically Treated Copper Surfaces, *Adv. Cryog. Eng.* **27**, 309 (1982).
30. Lehangre, J. C. Boissin, C. Johannes, and A. de La Harpe, Critical Nucleate Boiling of Liquid Helium in Narrow Tubes and Annuli, *Proceedings of the 2nd International Cryogenics Engineering Conference*, p. 274, Hiffe Science and Technology, Brighton, 1968.
31. M. N. Wilson, Heat Transfer to Boiling Liquid Helium in Narrow Vertical Channels, Liquid Helium Technology, *Proceedings of the International Institute of Refrigeration*, Commission 1, Boulder, CO, Pergamon Press, Oxford, 1966, pp. 109–114.

32. R. G. Sydoriak and T. R. Roberts, Study of Boiling in Short Narrow Channels and Its Application to Design of Magnets Cooled by Liquid $H_2$and N_2, *J. Appl. Phys*. **28**, 143 (1956).
33. Z. Chen and S. W. Van Sciver, Channel Heat Transfer in He I–Steady State Orientation Dependence, *Adv. Cryog. Eng*. **31**, (1986).
34. R. F. Barron, *Cryogenic Heat Transfer*, Taylor Francis, Philadelphia, 1999.
35. P. Giarratano, V. D. Arp, and R. V. Smith, Forced Convection Heat Transfer to Supercritical Helium, *Cryogenics* **11**, 385 (1971).
36. A. de La Harpe, S. Lehongre, J- Mollard, and C. Johannes, Boiling Heat Transfer and Pressure Drop of Liquid Helium I Under Forced Circulation in a Helically Coiled Tube, *Adv. Cryog. Eng*. **14**, 170 (1963).
37. C. Johannes, Studies of Forced Convection Heat Transfer to Helium I, *Adv. Cryog. Eng*. **17**, 352 (1972).
38. W. G. Steward, Transient Helium Heat Transfer Phase I–Static Coolant, *Int. J. Heat Mass Transfer* **21**, 863 (1978).
39. C. Schmidt, Transient Heat Transfer and Recovery Behavior of Superconductors, *IEEE Trans. Magnet*. **Mag-17**, 738 (1981).

Further Readings

R. F. Barron, *Cryogenic Heat Transfer*, Taylor Francis, Philadelphia, 1999.
A. Bejan, *Convection Heat Transfer,* Wiley, New York, 1984.
E. R. G. Eckert and R. M. Drake, *Analysis of Heat and Mass Transfer*, McGraw–Hill, New York, 1972.
J. Frenkel, *Kinetic Theory of Liquids*, Chap. 7, Dover, New York, 1955.
W. Frost, *Heat Transfer at Low Temperatures,* Plenum Press, New York, 1975.
F. P. Incropera and D. P. Dewitt, *Fundamentals of Heat Transfer*, Wiley, New York, 1981.
L. S. Tong, *Boiling Heat Transfer and Two Phase Flow*, Wiley, New York, 1965.
P. B. Whalley, *Two Phase Flow and Heat Transfer*, Oxford Science, Oxford, 1996